Marine Geology 255 (2008) 64–82

Contents lists available at ScienceDirect

Marine Geology

journal homepage: www.elsevier.com/locate/margeo

The last reconnection of the Marmara Sea (Turkey) to the World Ocean: A paleoceanographic and paleoclimatic perspective

Cecilia M.G. McHugh [a,b,*], Damayanti Gurung [a], Liviu Giosan [c], William B.F. Ryan [b], Yossi Mart [d], Ummuhan Sancar [e], Lloyd Burckle [b], M. Namik Çagatay [e]

[a] Queens College, The City University of New York, Flushing, NY, USA
[b] Lamont-Doherty Earth Observatory of Columbia University, Palisades, NY, USA
[c] Woods Hole Oceanographic Institution, Woods Hole, MA., USA
[d] Recanati Institute for Marine Studies, University of Haifa, Haifa, Israel
[e] Istanbul Technical University, Faculty of Mines, Ayazaga, Istanbul, Turkey

ARTICLE INFO

Article history:
Received 1 October 2007
Received in revised form 9 July 2008
Accepted 11 July 2008

Keywords:
late Pleistocene–Holocene
Marmara Sea
sea-level
paleoshorelines
Black Sea
Mediterranean Sea

ABSTRACT

During the late glacial, marine isotope Stage 2, the Marmara Sea transformed into a brackish lake as global sea-level fell below the sill in the Dardanelles Strait. A record of the basin's reconnection to the global ocean is preserved in its sediments permitting the extraction of the paleoceanographic and paleoclimatic history of the region. The goal of this study is to develop a high-resolution record of the lacustrine to marine transition of Marmara Sea in order to reconstruct regional and global climatic events at a millennial scale. For this purpose, we mapped the paleoshorelines of Marmara Sea along the northern, eastern, and southern shelves at Çekmece, Prince Islands, and Imrali, using data from multibeam bathymetry, high-resolution subbottom profiling (chirp) and ten sediment cores. Detailed sedimentologic, biostratigraphic (foraminifers, mollusk, diatoms), X-ray fluorescence geochemical scanning, and oxygen and carbon stable isotope analyses correlated to a calibrated radiocarbon chronology provided evidence for cold and dry conditions prior to 15 ka BP, warm conditions of the Bolling-Allerod from ~15 to 13 ka BP, a rapid marine incursion at 12 ka BP, still stand of Marmara Sea and sediment reworking of the paleoshorelines during the Younger Dryas at ~11.5 to 10.5 ka BP, and development of strong stratification and influx of nutrients as Black Sea waters spilled into Marmara Sea at 9.2 ka BP. Stable environmental conditions developed in Marmara Sea after 6.0 ka BP as sea-level reached its present shoreline and the basin floors filled with sediments achieving their present configuration.

1. Introduction

Reconnections of marginal basins to the World Ocean after the late glacial eustatic low stand can help track global sea-level rise due to the amplified sedimentation changes and complete replacement in the fauna and flora that occurs when these basins switch from lacustrine to marine conditions. Intracontinental basins tend to be small and respond to environmental changes rapidly. Therefore such basins have the potential to capture high-resolution regional and global paleoclimatic and paleoceanographic variability in their sedimentary records (Leventer et al., 1982; Thunell and Williams, 1989; Peterson et al., 1991; Behl and Kennett, 1996; Hughen et al., 1996; Sidall et al., 2003; Ortiz et al., 2004; Major et al., 2006).

The Marmara Sea is an intracontinental basin 275 km long and 80 km wide formed as a result of pull-apart tectonics along the North Anatolia Fault (Fig. 1; Sengör et al., 1985; Görür et al., 1997; Armijo et al., 1999, 2002, 2005; Okay et al., 1999; Le Pichon et al., 2001; Demirbag et al., 2003). The geological evolution of the Marmara Sea began in the Neogene, late Serravallian, Miocene, and possibly as late as the Plio-Pleistocene. Marmara Sea is divided into three major sub-basins, named Tekirdag, Central, and Çinarcik, from west to east, that are ~1200 m deep. Saddles as shallow as 400–600 mbsl separate these basins (Fig. 1). The northern shelf of Marmara Sea is narrow (~15 km). In contrast, the southern shelf is as broad as 50 km. The dimensions of the drainage basins and river discharge are quite different on the northern and southern margins. To the north the drainage basin is 4438 km^2 in extent, and there are only small streams with no significant discharge (Okay and Ergun, 2005). In contrast, the drainage to the southern margin extends over an area of 30,600 km^2 and drains several medium-sized rivers with a total sediment delivery of 6.3×10^6 tons/yr (Ergin et al., 1991).

The Marmara Sea is connected to the Aegean Sea through the Dardanelles Strait (Görür et al., 1997; Çagatay et al., 1999, 2000). Recent

* Corresponding author. Queens College, The City University of New York, Flushing, NY, USA.
E-mail addresses: cmchugh@qc.cuny.edu, cecilia@ldeo.columbia.edu (C.M.G. McHugh).

0025-3227/$ – see front matter © 2008 Elsevier B.V. All rights reserved.
doi:10.1016/j.margeo.2008.07.005

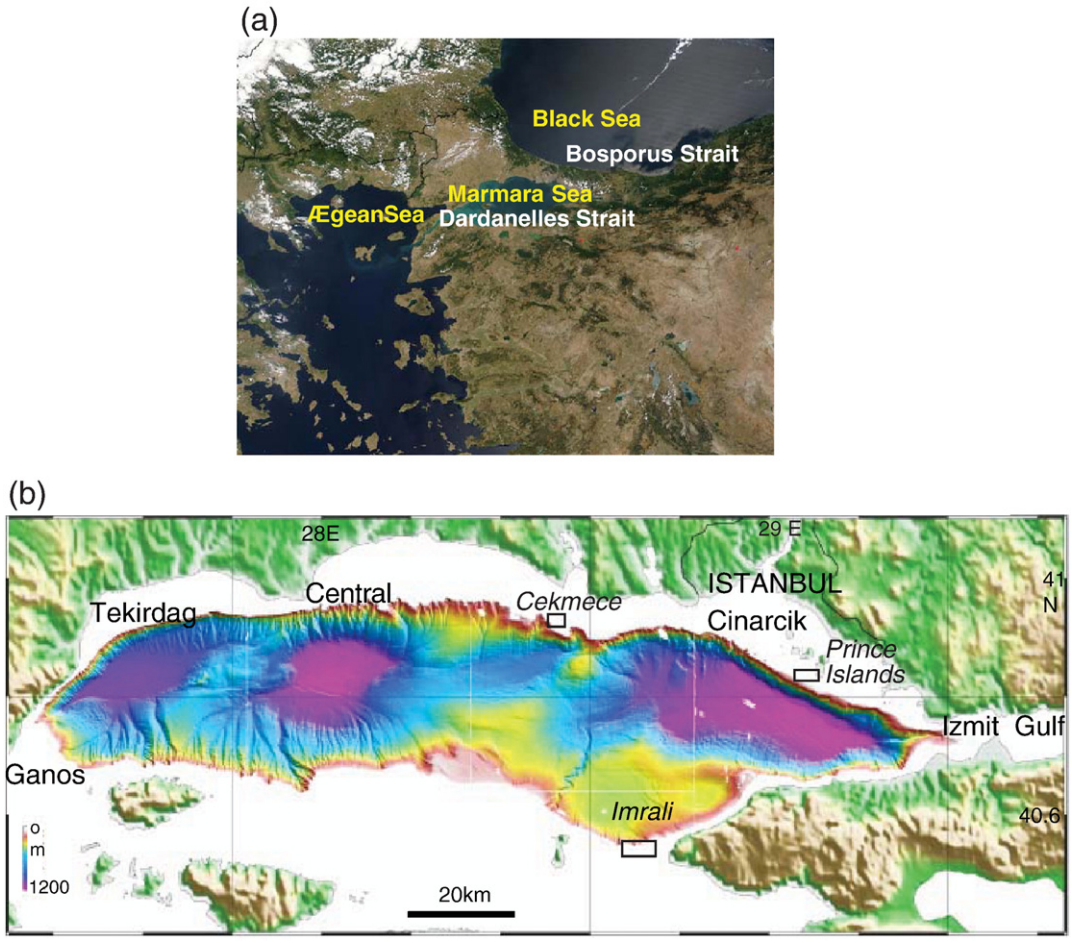

Fig. 1. (a). Satellite image of the Aegean Sea, Marmara Sea and Black Sea corridor showing Marmara's significant location as a gateway between the Aegean and Black Seas, and the location of the Dardanelles and Bosporus Straits. (b) Multibeam bathymetry of the main Marmara Sea basins (Rangin et al., 2001). Boxes show the location of the studied areas in Imrali, Prince Islands and Çekmece shelves.

studies by Gökasan et al. (2008) showed that the Dardanelles Strait is 74 km long, 1.3 to 7.5 km wide with average water depths of −60 m. During the last glacial when Marmara Lake was isolated from the Mediterranean Sea, water depths along the Dardanelles Strait averaged −85 m (Gökasan et al., 2008). Marmara Sea is connected to the Black Sea through the Bosporus Strait (Gökasan et al., 1997, 2005). The Strait is 31 km long, and its width varies from 0.7 to 3.5 km (Algan et al., 2001; Gökasan et al., 1997, 2005). Sills located at the southern and northern entrances of the Bosporus Strait are −35 m and −58 m deep, respectively. The basement topography is irregular and characterized by sills of −120 m to the south and −80 m to −70 m towards the north.

The oceanography of the Marmara Sea is characterized by the outflow of brackish water from the Black Sea with salinity of 18‰ and inflow of saline intermediate and bottom water (38‰) from the Aegean Sea (Besiktepe et al., 1994). Water and suspended sediments are delivered to Marmara Sea from the Straits of Dardanelles and Bosporus. These straits help maintain the balance between water supply and evaporation. The flux rate of suspended solids for the Dardanelles Strait is 9.0×10^5 tons/yr and for the Bosporus Strait, 14.5×10^5 tons/yr (Ergin et al., 1991). During the last glacial, marine isotope Stage 2, when global sea-level dropped below the −85 m Dardanelles Sill, Marmara lost its connection from the global ocean and became a fresh–brackish water lake (Stanley and Blanpied, 1980; Ryan et al., 1997, 2003; Aksu et al., 1999, 2002; Çagatay et al., 1999, 2000). Although the reconnection of Marmara Sea to the Mediterranean Sea has been previously documented, questions remain regarding the level of Marmara Lake at the time of marine incursion and whether the Black Sea outflow to Marmara was vigorous and continuous at the time of the reconnection (Ross and Degens, 1974; Stanley and Blanpied, 1980; Lane-Serff et al., 1997; Aksu et al., 1999, 2002; Kaminski et al., 2002; Mudie et al., 2002) or discontinuous (Ryan et al., 1997, 2003; Major et al., 2002, 2006; Myers et al., 2003; Sperling et al., 2003; Giosan et al., 2005). Due to its irregular basement topography and sediment thicknesses, there are questions as to whether the depth of the Bosporus Strait was shallow or deep during the reconnections. Some authors have concentrated on characterizing the stratigraphy, sediment infill, delta formation, and physical oceanography to shed light into this problem (Ergin et al., 1991; Algan et al., 2001; Hiscott et al., 2002; Myers et al., 2003; Sidall et al., 2004; Gökasan et al., 1997, 2005; Eris et al., 2007).

This study uses geophysical, sedimentological, biostratigraphic, physical and geochemical data, as well as stable isotopes obtained from foraminifera to document the reconnection of Marmara Lake to the global ocean and to address the following questions. 1) Was the surface of the Marmara Lake below its outlet to the Aegean Sea just prior to the reconnection? If so, was this indicative of regional drought conditions? 2) Was the Marmara Lake isolated from the Black Sea during its reconnection to the global ocean? 3) Was the incursion of marine waters in the brackish–fresh water lake rapid and accompanied by extensive changes in paleodepositional environments (i.e., the migration of the shoreface and drowning of river beds), faunal (mollusks, foraminifers) and floral (diatom) assemblages? 4) What paleoclimatic and paleoceanographic events can be detected in the lake and marine records and can these events be recognized at millennial-scale variability?

The data that forms the basis for this study was collected during geophysical surveys and sediment sampling conducted from the *R/V Mediterranean Explorer* in the summer of 2005 (Fig. 1; Mart et al., 2006) and from the *R/V Urania* in 2001 (Çagatay et al., 2003; Polonia et al., 2004; Cormier et al., 2006). We mapped the paleoshorelines of Marmara Lake along the northern, eastern, and southern shelves at Çekmece, Prince Islands, and Imrali, respectively. Multibeam bathymetry, high-resolution subbottom profiling (chirp) and sediment cores were obtained from present water depths of −75 to −300 m.

2. Methods

The *R/V Mediterranean Explorer* geophysical survey was conducted with an EdgeTech SB424 chirp reflection profiler navigated by GPS. N–S and E–W track lines were separated at 0.1' spacing (185–150 m). Each surveyed area was approximately 4 by 6 km wide. The digital field data were sampled at a 0.125 ms interval across a 0.2 s window and recorded in EdgeTech format. The files were converted to SEGY format for shipboard analysis with the TKS Kingdom Suite® software package. Gravity coring was conducted with a 10 cm diameter and up to 3 m long barrel with a 400 kg core head. The *R/V Mediterranean Explorer* sediment cores were recovered from the Çekmece and Prince Islands margins. The cores were split, photographed, described and sampled in the ship's laboratory. U-channels were taken from each 1.5 m core section for bulk X-ray fluorescence (XRF) geochemical scanning conducted every 1 mm along the sediment surface. Bromine relative content (in counts/second), as measured by the XRF scanner, was used to estimate the presence of marine organic matter in the sediments. Bromine is thought to be preferentially associated to marine rather than freshwater-derived organic matter (Malcolm and Price, 1984). The calcium carbonate content of the sediments was measured every 5 cm using a Coulometric carbonate–carbon analyzer. The accuracy of this method was +/-0.05%. Carbonate content is expressed as wt.% $CaCO_3$, assuming that all the carbonate was present as calcite. Cores are archived (one half each) at the Istanbul Technical University and the University of Haifa.

High-resolution multibeam (ELAC1180 system) and subbottom CHIRP profiling (hull mounted Datasonics) conducted at 50 m spaced grids, were obtained from the *R/V Urania* in the summer of 2001 (Çagatay et al., 2003; Polonia et al., 2002, 2004; Cormier et al., 2006). Precise navigation was provided by differential GPS positioning and bathymetric maps are referenced to the WGS84 datum. The physical properties of the cores were measured on board of the *R/V Urania* with a Geotech core logger (Polonia et al., 2002). The studied gravity cores IM03 and IM05 were recovered from the Imrali margin from the *R/V Urania*. To recover the water and undisturbed underlying sediment, the SW-104 coring system was used.

Oxygen isotopes were conducted at the Woods Hole Micropaleontology Mass Spectrometer Facility with a Finnegan MAT253 mass spectrometer from the tests of the benthic marine foraminifer *Brizalina* spp. A chronology was established from ^{14}C derived from mollusks and foraminifers (Table 1). Radiocarbon dating was conducted at the NOSAMS Facility at Woods Hole, MA. Given the great variability in water masses of the Marmara Sea ages are reported as both calibrated years BP and radiocarbon years BP (Table 1). Calibrated ages were obtained by applying Siani et al. (2000) reservoir correction. The ages were converted to calendar years with CALIB 5.0 program (Stuvier and Reimer, 1993). All the cores identification, water depth and coordinates are described in Table 2 in the Supplementary Data.

All sediment cores were sampled every 5 cm for foraminiferal and mollusk biostratigraphy, except for Cores IM03 and Core 8 that were sampled every 10 cm (Gurung et al., 2006). All the samples were wet sieved through a 63 μm sieve and the fractions of the sample >63 μm were dried and picked for analyses. Mollusks were identified to genus level using Abbott and Dance (1990) and Vaught et al. (1989) and 22 genera were identified. The dominant taxa that were considered before the marine incursion are fresh–brackish mollusks of Caspian affinity and characteristic of Neoeuxinian Black Sea sediments *Dreissena* sp. and *Theodoxus* sp. (Fedorov, 1971; Ross and Degens, 1974). After the marine intrusion the molluskan fauna is indicated by shallow littoral marine species of Mediterranean affinity *Gouldia* sp., *Lucinella* sp., *Corbula* sp., *Cardium* sp. (Tables 3–11 in Supplementary Data). Foraminifers, at least 300, were picked from 10 g sub-samples, identified to genus level with a binocular microscope, counted, and standardized by calculating percent abundance within each sample (Tables 12–21 in Supplementary Data). Benthic foraminiferal species were identified and counted for Core IM05, and Mediterranean Explorer Cores 6, and 1 on the southern (Imrali), northern (Çekmece), and Prince Islands margins of Marmara Sea (Taxonomy in Appendix A). These cores were chosen to identify species because of their continuous sedimentation as documented by the lithostratigraphy and radiocarbon chronology. Foraminiferal taxonomy is based on Loeblich and Tappan (1988). Further identification to genera and species level was carried out by using Phleger (1960), Murray (1971, 1986), Haynes (1981), Yanko and Troitskaja (1987), Alavi (1988), Cimmerman and Langer (1991), Sgarella and Moncharmont Zei (1993), Lee et al. (2000), Kaminski et al. (2002), Hayward et al. (2003), and Meric et al. (2004).

Samples for diatom studies were taken every 5 cm in Core IM05 and every 10 cm for Core IM03, chemically treated with 10% hydrogen peroxide and 10% hydrochloric acid to extract the diatoms, and thin sections were prepared without heating the samples. The method used represents a slight modification from Renberg (1990). Two hundred diatom valves were counted from each interval, identified to the genus level using Round et al. (1990) and grouped into: freshwater, brackish, and marine (Table 22 in Supplementary Data). Fresh and brackish water diatoms are better preserved in the sediments because they have thick-walls. In contrast marine diatoms are thinner walled, more susceptible to dissolution and not well preserved. The absence of all

Table 1
Radiocarbon and calibrated ages for the studied cores

Core I.D.	Depth mbsf	Core int. (cm)	Type	Mollusk	^{14}C age	Age error	Calibrated age[a] (ka)
MedEx05-1	102.60	60	Mollusk	*Corbula* sp.	10,600	45	11.73
MedEx05-1	102.95	95	Foraminifera		9910	60	10.74
MedEx05-1	103.00	100	Mollusk	*Corbula* sp.	10,500	50	11.52
MedEx05-2	93.95	30	Mollusk	*Lucinella* sp. *Gouldia* sp.	8760	55	9.36
MexEx05-3	93.20	20	Mollusk	*Lucinella* sp. *Gouldia* sp.	5000	40	5.26
MexEx05-3	93.25	25	Mollusk	*Lucinella* sp. *Gouldia* sp.	10,300	50	11.21
MedEx05-3	93.50	50	Foraminifera		6900	35	7.35
MexEx05-5	93.00	70	Mollusk	*Lucinella* sp. *Gouldia* sp.	9890	50	10.70
MexEx05-5	93.10	80	Mollusk	*Lucinella* sp. *Gouldia* sp.	10,450	80	11.46
MedEx05-6	98.5	100	Foraminifera		5350	45	5.64
MedEx05-6	99.10	160	Foraminifera		9280	60	10.00
MedEx05-6	99.25	175	Mollusk	*Lucinella* sp. *Gouldia* sp.	9720	55	10.50
MedEx05-6	99.52	202	Mollusk	*Corbula* sp.	10,600	40	11.74
Core IM03	299.60	150	Foraminifera		5260	50	5.50
	300.40	230	Foraminifera		5420	80	5.72
Core IM05	152.15	55	Foraminifera		3440	25	3.24
	152.60	100	Foraminifera		4700	40	4.85
	152.60	200	Foraminifera		8590	40	9.15
	154.05	245	Mollusk	Clam	11,500	75	12.95[b]
	154.15	254	Foraminifera		10,350	45	11.25
	154.21	260	Mollusk	Clam	10,650	40	11.83
	154.55	295	Mollusk	*Dreissena* sp.	13,000	65	14.66
	155.14	354	Mollusk	*Dreissena* sp.	13,150	60	14.95

[a] Calibrated ages were obtained by applying Siani et al. (2000) reservoir corrections and converted to calendar years with the CALIB 5.0 program (Stuvier and Reimer, 1993).
[b] Possibly reworked.

diatoms in the sediments that contain marine foraminiferal and mollusk assemblages is interpreted as the result of dissolution rather than low productivity.

3. Results

3.1. Southern shelf at Imrali

The Imrali shelf-slope region along the Southern Boundary Fault was surveyed between −80 m and −300 m of water depth (Fig. 2). The goal of the survey was to document neotectonic activity along the Southern Boundary Fault and to map the paleoshorelines. The topography of the surveyed region, has a steep slope (up to 20°) that subbottom profile records show was created by normal fault activity and a series of rotational slumps concave to the basin (McHugh et al., 2006; Fig. 2). A transect of cores was obtained extending from present water depths of −100 to −300 m. Core IM05 was recovered from 152 m of water depth at the base of one of these scarps. After reconstruction of the 30 m of vertical offset during the Holocene (past 10,000 yr) due to faulting and slumping processes, Core IM05 was positioned at −115 m of present water depth (McHugh et al., 2006; Fig. 3). The reconstruction was based on the identification of the seismic reflector that represents the lacustrine to marine transition from the lithology, biostratigraphy and radiocarbon dating. The vertical offsets were measured from the seismic lines and the seismic reflector reconstructed to its original position. Core IM03 was taken at −298 m of water depth, 1 km away from the fault, and its sediments were not offset by fault activity. Three terraces were delineated from the reconstructed subbottom profiles at −87 m, −95 m, and −115 m of water depth (Fig. 3).

3.2. Sediments, flora, mollusks

Core IM05 was subdivided into four sedimentary facies based on its texture, flora, and fauna (Fig. 4). Facies 1: lacustrine-barren is composed of laminated silty clays with abundant woody material and rare fragments of Neoeuxinian–Caspian affinity mollusks of *Dreissena rostriformis* and the gastropod *Theodoxus fluviatilis* (Fedorov, 1971; Ross and Degens, 1974). Sediments of Facies 1 are older than 15.0 ka BP (13.15 ^{14}C ka BP). Facies 2: lacustrine-fertile is composed of silty clays with abundant mollusks dominated by *Dreissena* sp. banks and also by the gastropod *T. fluviatilis*. These two assemblages were typical of brackish water environments with salinities of 1–5‰. The lake sediments of Facies 2 also contain brackish water diatoms *Cyclotella* spp; *Cocconeis* spp; *Diploneis* spp. and *Amphora* spp. and freshwater diatoms *Stephanodiscus* spp; *Fragilaria* spp; *Eunotia* spp; *Navicula* spp; *Cymbella* spp; *Cystopleura* spp. During the lake-fertile stage sedimentation rates were as high as 0.4 cm/yr (Fig. 5). Sediments of Facies 2 were deposited between 15.0 to 12.0 ka BP (13.15 ^{14}C ka BP and 11.0 ^{14}C ka BP; Table 1). Facies 3 represents the marine incursion surface and is composed of a 20 cm-thick gravelly sand bed containing flat pebbles typical of a beach environment. A marine mollusk above the sand bed was dated at 11.8 ka BP (10.7 ^{14}C ka BP). Facies 3 separates lacustrine from marine strata and marks a major transformation in the sediments, flora and fauna. Facies 4 is entirely composed of marine sediments and fauna. The sediments are clayey silts and contain marine mollusks, marine benthic and planktonic foraminiferal assemblages. Marine diatom tests were rarely preserved in the sedimentary record due to their dissolution in the water column. Sediments of Facies 4 were deposited from 11.83 ka BP (10.7 ^{14}C ka BP) to the present. Sedimentation rates for

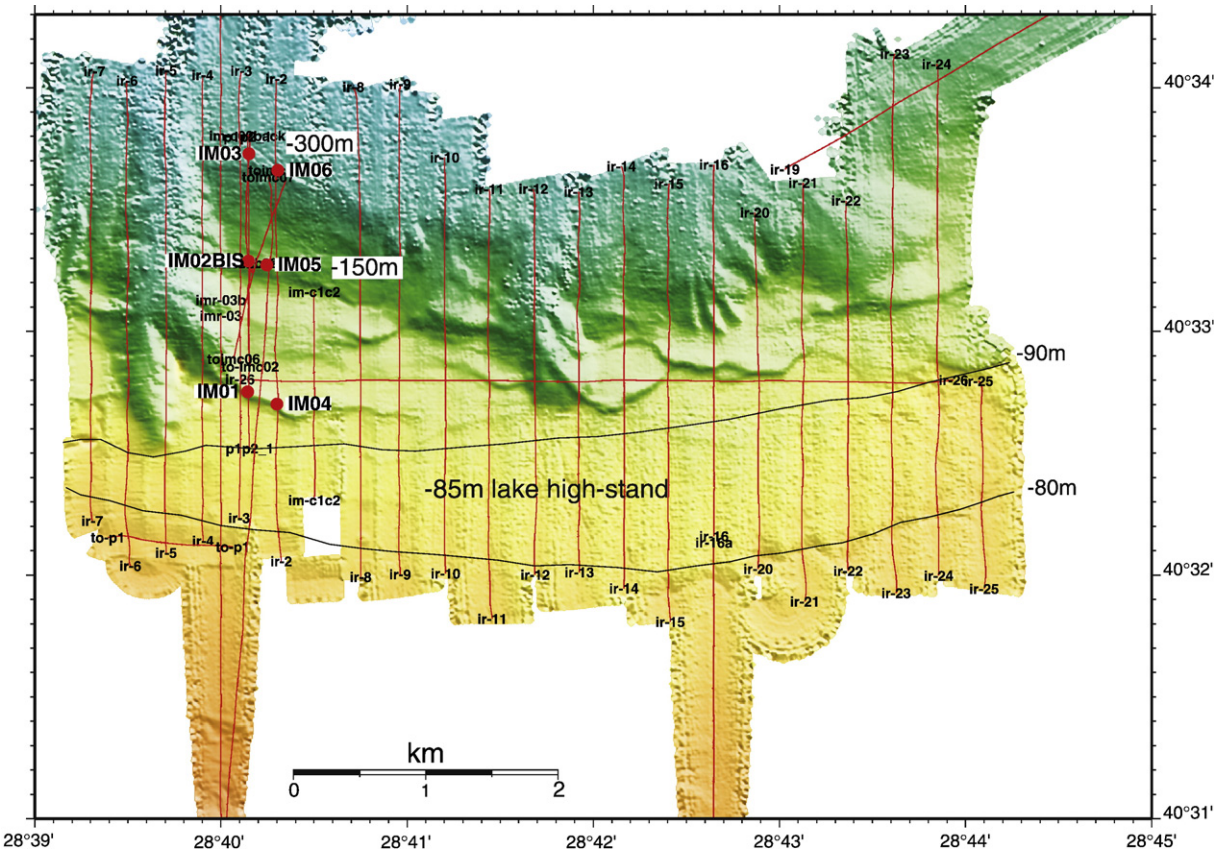

Fig. 2. Multibeam bathymetry of the Imrali study area showing the location of high-resolution subbottom profiles, CHIRP, navigation tracks (red lines) and location of core transect (red dots). The studied cores IM05 and IM03 are located at −152 and −298 m of water depth, respectively. The Marmara Lake high-stand was at −85 m (Çagatay et al., 2000; Algan et al., 2001; Newman, 2003).

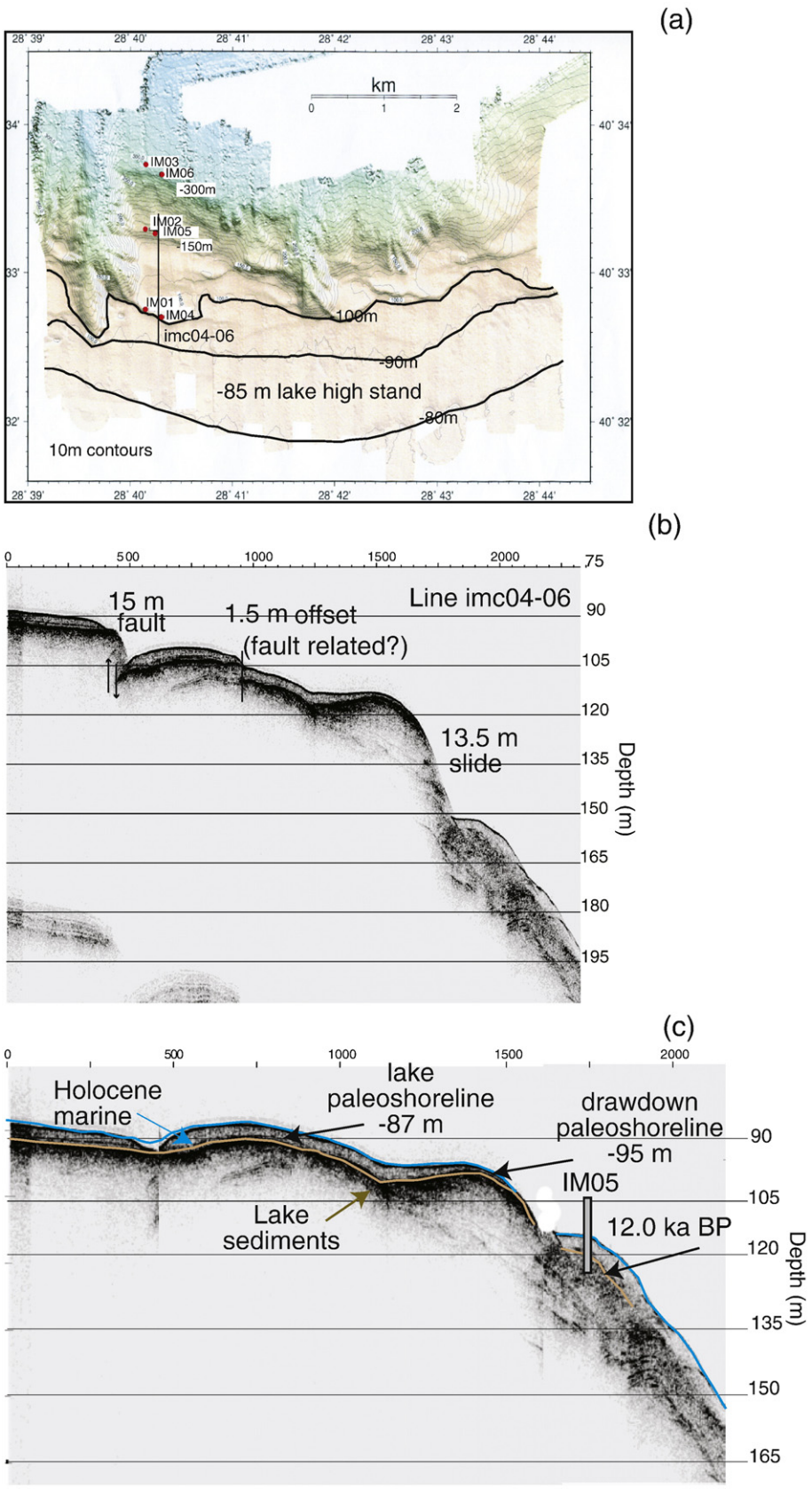

Fig. 3. (a). Multibeam bathymetry of the Imrali study area showing the location of the cores and CHIRP subbottom profile (Line imc04-06). Modified after McHugh et al., 2006. (b). CHIRP subbottom profile extending from −90 to −200 m. Offsets due to normal fault activity are 15 m and 1.5 m. Also shown an offset of 13.5 m due to possibly slumping and/or related fault activity. (c). After reconstruction of fault related offsets, Core IM05 is located at −115 m, there is a paleoshoreline at −95 m, and the lake high-stand paleoshoreline at −87 m. Correlation of the lithology and age to the seismic line reveals the lacustrine–marine transition occurred at ~12.0 ka BP (brown reflector). Turquoise surface delineates the sea-floor and sediment deposited during the Holocene.

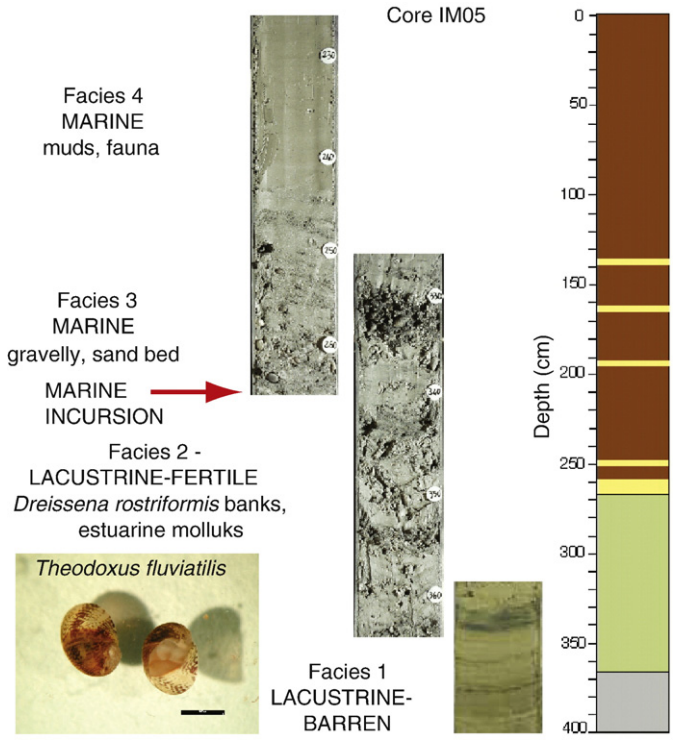

Fig. 4. Lithology and facies of Core IM05 showing the lacustrine-barren stage (Facies 1, 400–365 cm) and lacustrine-fertile (Facies 2, 365–275 cm). The transition from lacustrine to marine (Facies 3) is marked by a bed of coarse sand with flat, well-rounded pebbles, and sand laminae above (275 to 260 cm). Marine muds and fauna characterize the core from 260 to 0 cm (Facies 4).

the marine facies were very stable at 0.02 cm/yr (Fig. 5). Core IM03 is composed of marine muds and marine fauna and it is 350 cm long. No diatoms were found in Core IM03. The lower section of Core IM03 is laminated and the sparse occurrence of benthic and planktonic foraminifers suggests that its base was very close to the lake sediments. Core IM03 was dated at 5.7 ka BP (5.4 ^{14}C ka BP) at 230 cm and 5.5 ka BP (5.3 ^{14}C ka BP) at 150 cm and correlated to Core IM05 based on the radiocarbon ages (Table 1).

3.3. Physical properties

The bulk density, p-wave velocity and magnetic susceptibility of the sediments were measured on cores IM05 and IM03. They showed an abrupt change at the contact between the lacustrine and marine facies (Fig. 6). The bulk density measurements increased upwards in the core from 1.9 g/cm^3 in the lacustrine-barren Facies 1 to 2.3 g/cm^3 in the lacustrine-fertile Facies 2. These high values of bulk density in the lacustrine facies are indicative of low pore water content. In the upper marine part of the core (Facies 4) bulk densities decrease further to values of 1.55 g/cm^3 that are typical of water-saturated surface sediments. The abrupt contact between the lacustrine and marine facies is also accompanied by a decrease in the p-wave velocity from 1650 m/s to 1550 m/s. The magnetic susceptibility values also exhibited changes from the lacustrine to the marine facies with highest susceptibility at 25 cm and 140 cm below the contact.

3.4. Benthic and planktonic foraminifers

All shelf-slope cores from the southern Marmara margin at Imrali and northern margin at Prince Islands and Çekmece contain similar benthic foraminiferal assemblages (Fig. 7; Gurung et al., 2006). The record of benthic foraminifers in the outer shelf was appropriate for environmental analyses because benthic foraminifers respond rapidly to changing conditions such as deepening, sediment supply, organic matter, and oxygen concentrations (Sen Gupta and Machain-Castillo, 1993; Sen Gupta et al., 1996). For this study we classified benthic foraminifers based on Murray (1991, 2006), Kaiho (1994), Cannariato et al. (1999), Kaminski et al. (2002) and Meric and Algan (2007) into two major subgroups: 1) low oxygen concentrations or suboxic: *Brizalina* spp., *Bulimina* spp., and *Cassidulina* spp., and 2) shallow water, tolerant of a wide range in salinity: *Elphidium* spp. and *Ammonia* spp. Some species such as *Hyalinea* spp. and *Globobulimina* spp. reflect the development of water stratification and high organic carbon flux in shelf environments and have been used to interpret these environmental conditions (Murray 1991, 2006; Schonfeld, 1997, 2001; den Dulk et al., 2000; Evans et al., 2002; Fontanier et al., 2002, 2003).

Twenty benthic foraminiferal species were found in Core IM05 that indicate changes of salinity, water depth, deepening and development of stratification in the water column. Benthic foraminiferal assemblages were first established during the initial incursion of marine waters at around 12.0 ka BP (10.7 ^{14}C ka BP). From 12 ka BP to 11.0 ka BP *Cassidulina carinata* and then *Brizalina* spp. (*B. catanensis*, *B. spathulata*) were the first marine foraminifers present in the sedimentary record of IM05. Except for the initial marine incursion in which only two species were dominant *Brizalina* spp. (*B. catanensis*, *B. spathulata*, *B. alata*, *B. striatula*) exhibited similar patterns throughout the core and has been grouped by genus. The species *Ammonia tepida*, *E. macellum*, and *E. articulatum* were also present during the initial marine incursion, from 12 ka BP to 11.0 ka BP, and they indicate that the sediments were deposited in a shallow water environment with a wide range in salinity conditions (Debenay et al., 1998; Murray, 2006; Meric and Algan, 2007; Fig. 7). *E. macellum* is characteristic of seagrass, marsh assemblages further suggesting nearshore environment (Murray, 1991).

The relative abundances of *C. carinata*. and *Brizalina* spp. decreased from 11.5 ka BP to 10.0 ka BP and benthic foraminiferal species were dominated by *Bulimina aculeate*. *Bulimina* spp. (*B. aculeate*; *B. costata*; *B. marginata*; *B. elongata*) behaved in a similar patter throughout the rest

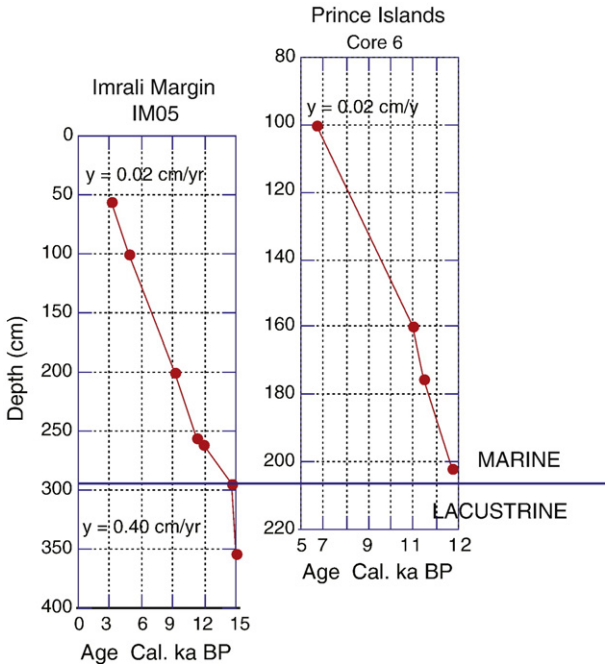

Fig. 5. Sedimentation rates calculated from the slope of the line for Core IM05 and Core 6 on the Imrali and Prince Islands margin, respectively. Sedimentation rates for the lacustrine stage are two orders of magnitude greater than the marine. Sedimentation rates for the Holocene are comparable for the southern and northern margins.

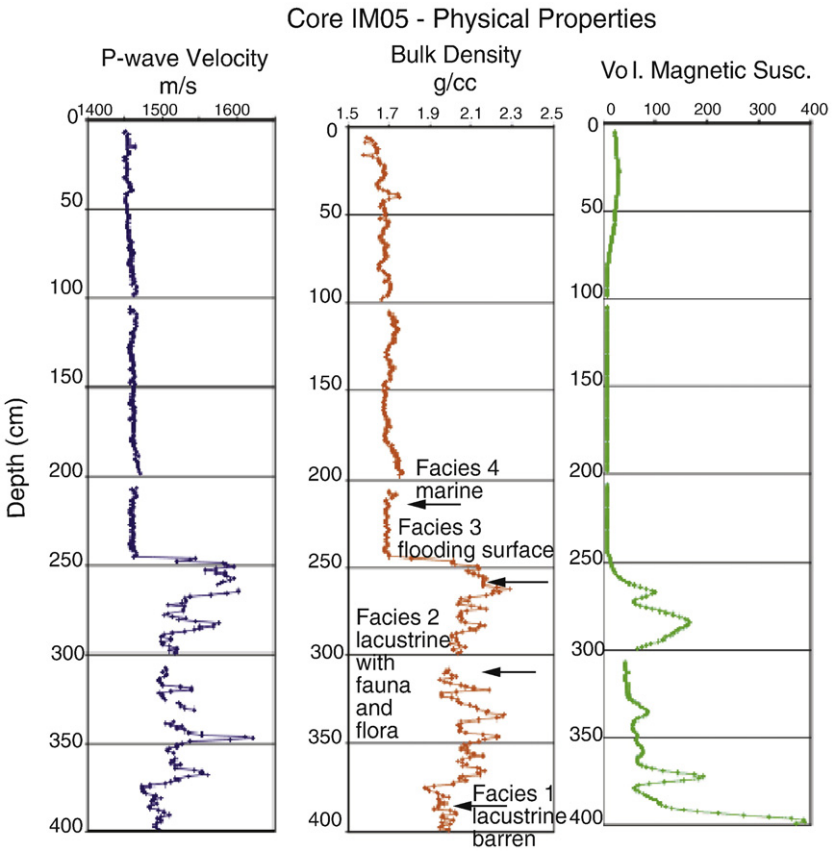

Fig. 6. The physical properties of Core IM05 (p-wave velocity, bulk density, and magnetic susceptibility) show the changes that occurred from the barren lake stage (Facies 1), to the fertile lake (Facies 2), due to the marine incursion (Facies 3), and after fully marine conditions were established (Facies 4).

of the core and was grouped by genus. Deepening was manifested by the near disappearance of the shallow water species *Elphidium* spp. and *A. tepida* and by the appearance of planktonic foraminifers at ~11.0 ka BP. *Hyalinea balthica* made its first appearance at ~11.0 ka BP. *H. balthica* has been interpreted as an indicator for the onset of stratification in the water column in other shelf settings (Scourse et al., 2002; Evans et al., 2002; Murray 2006). Large increases of specimens of *H. balthica* occurred at 9.1 ka BP and ~6.0 ka BP and they are interpreted as having been produced by outflow of Black Sea waters, and due to deepening as sea-level reached near its present position, respectively. *Globobulimina*

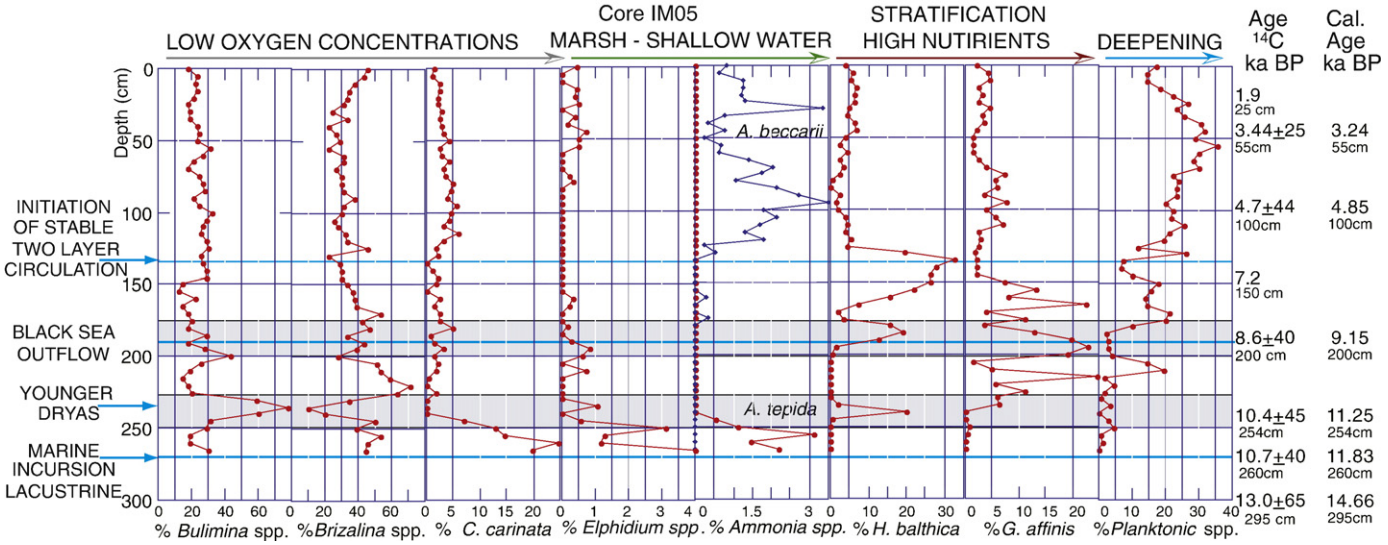

Fig. 7. Benthic and planktonic foraminiferal assemblages from the Imrali outer shelf exhibit major faunal and ecological shifts due to rapidly changing environmental conditions. Most foraminifers are grouped by genus due to the similar ecological preferences of species (*Bulimina* spp., *Brizalina* spp.) *A. tepida* is restricted to shallow water, marsh environments while *A. beccarii* is a highly adaptable species. *H. balthica* is associated to stratification of the water column. *G. affinis* equates with high organic flux and productivity. Ages are reported as radiocarbon, calibrated, and some (at 150 and 25 cm) were calculated from the sedimentation rates of 0.02 cm/yr.

affinis is associated to high organic flux (>3.5 g C m^{-2}/yr) tolerates dysoxia but can also be found under oxic conditions (Schonfeld, 1997, 2001; den Dulk et al., 2000; Fontanier et al., 2002, 2003; Murray 2006). Large increases in the abundance of *G. affinis* at ~10 ka BP, 9.1 ka BP and 8.0 ka BP are interpreted as influx of nutrients after the Younger Dryas, and outflow of Black Sea waters. After ~6.0 ka BP all benthic foraminifers showed little variability except for the appearance of *A. beccarii* a much more tolerant form of *Ammonia* spp. (Fig. 7; Thomas et al., 2000). The relative abundances of planktonic foraminifers decreased from 35% to 15% after 3.24 ka BP (Fig. 7).

3.5. Stable isotopes

The oxygen isotope record of cores IM05 and IM03 recovered at −150 and −300 m of water depth, respectively, showed values ranging from 2.2‰ $\delta^{18}O$ at ~12.0 ka BP to 1.5‰ $\delta^{18}O$ at present (Fig. 8a). Both cores showed a trend from heavy to light values that reflect high salinity and colder temperatures during the initial incursion of marine waters. The waters gradually freshened and warmed throughout the Holocene.

Carbon isotopes ranged from −2.5 to −0.5‰ $\delta^{13}C$ showing an overall trend to less depleted values. This could be related to a decrease in the organic matter flux and rates of sedimentation as Marmara Sea deepened and the shoreline approached its present position. The $\delta^{13}C$ values of IM05 and IM03 can be correlated in the upper meter of both cores from ~5.0 ka BP to the present, indicating that environmental conditions remained stable at both locations within the past 5.0 ka (Fig. 8b).

3.6. Eastern shelf at Prince Islands

The Prince Islands shelf was surveyed from −80 to −120 m of water depth (Fig. 9). The subbottom profile records showed a terrace at −93 m of water depth, deeper than the −85 m lake paleoshoreline, and of comparable depth to the paleoshoreline on the Imrali margin. Four cores were recovered from the shelf-slope boundary Core 7 at −88 m, Core 5 at −92 m, Core 6 at −98 m, and Core 8 at −109 m (Table 1; Fig. 9). The coring strategy was based on the expectation of reaching older strata that may have been truncated by erosion during the lake stage of Marmara for reconstructing the lacustrine to marine transition. The oldest sediments were expected to be at the shallowest depths where sub-aerial exposure of the shelf would have led to more erosion. The youngest sediments were expected to be at the deepest parts of the study area due to sediment progradation of younger strata over old, and to the generally better preservation of deeper strata. Cores 6–8 recovered marine sediments and Core 5 penetrated lacustrine strata (Figs. 10 and 11; Gurung et al., 2006). When compared to lacustrine values (Fig. 12), high Br content of over ~200 counts/s also indicated the presence of marine rather than fresh water-derived organic matter in the cores recovered in this region. Core 5 was dated at 10.7 ka BP (9.9 ^{14}C ka BP) at 70 cm and 11.5 ka BP (10.4 ^{14}C ka BP) at 80 cm. An age of 12.0 ka BP was estimated at 100 cm (Fig. 10). The base of Core 6 was dated from a marine mollusk at 11.7 ka BP (10.6 ^{14}C ka BP). Core 7 was very short (60 cm). We attributed this lack of penetration and sediment recovery to the stiffness of the low-water content lacustrine strata. The low-water content and high bulk density of the lacustrine substrate at or shallower than the present substrate at the −87.5 m isobath was most likely intermittently exposed when the Marmara Lake reached its low stand prior to 12 ka BP.

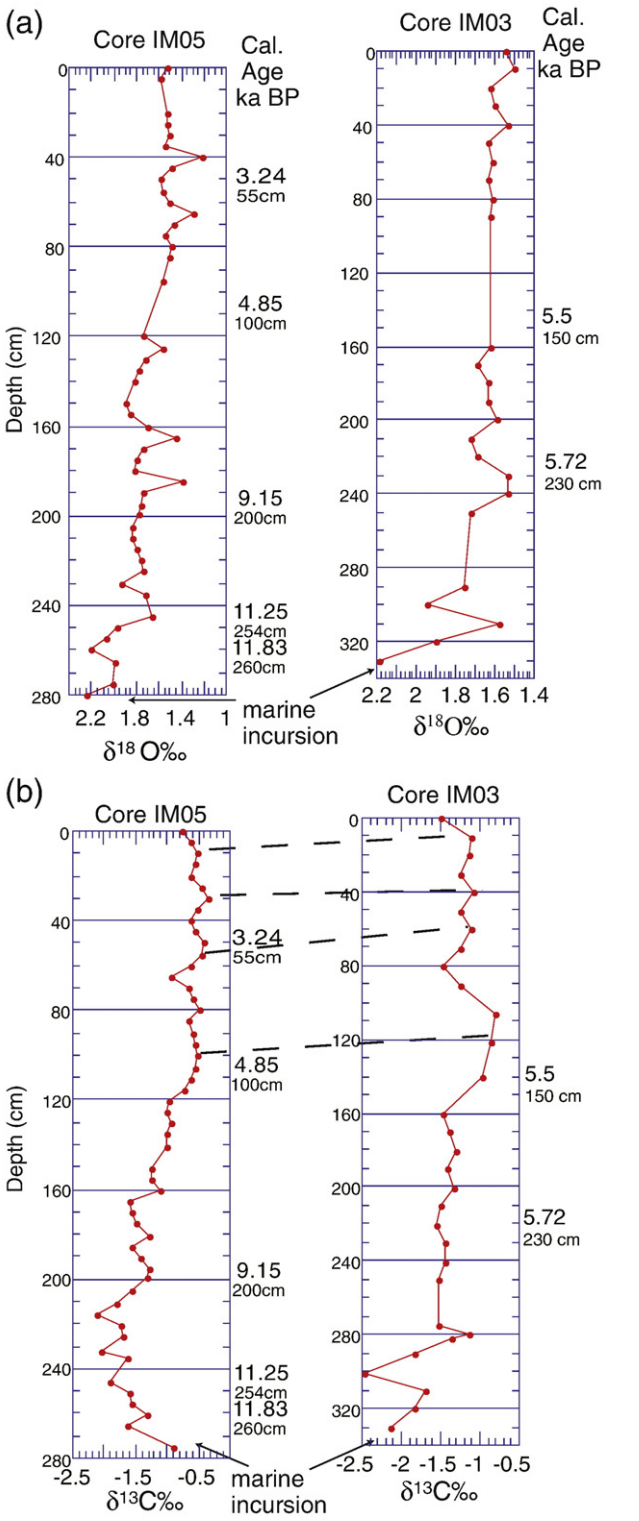

Fig. 8. (a). Stable oxygen isotope records of Cores IM05 and IM03. Ages are shown as calibrated years BP. Both cores isotope values range from 2.2 to 1.2 $\delta^{18}O$‰ and show an overall trend to lighter values interpreted as warming and freshening. Heavy values in both cores are interpreted as a high salinity and low temperature signal. (b). Correlation of carbon isotopes between Cores IM05 and IM03. Both cores show an overall trend to less depleted values from −2.5 to −0.5 $\delta^{13}C\delta^{13}C$ and uniform values after ~6 ka BP.

3.7. Sediments, mollusks

All four cores (5–8) were primarily composed of silty clay with sandy mud/muddy sand in the lower 30 cm (Fig. 10). Only Core 5 contained solely lacustrine mollusks at its base. All other cores contained reworked mollusk shells of both marine and fresh water affinity i.e., *Corbula* spp. and *Dreissena* spp., respectively, at the bottom suggestive that the marine–lacustrine transition was close but not recovered. Also present towards the base of the cores were charcoal

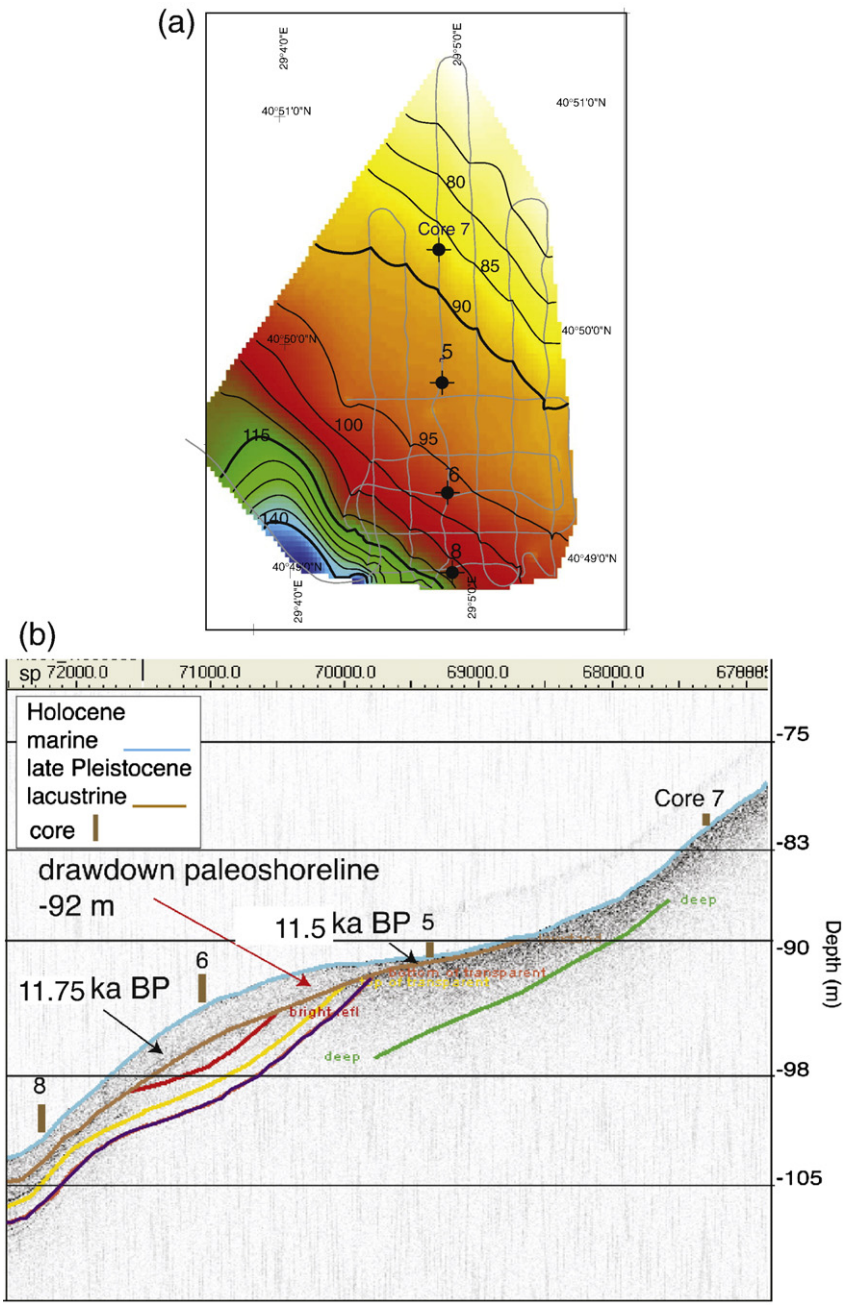

Fig. 9. (a). Sediment coring sites along the outer shelf of Prince Islands. Water depth contours are given in meters. (b). Subbottom profile (CHIRP) showing a −92 m terrace, lacustrine surface (brown), and marine Holocene sediments above (blue). The age of the sediments above the lacustrine surface, ~12 ka BP, is in calibrated years.

fragments, medium-grained, very well-sorted, and very well-rounded, black sands interbedded with intervals of very indurated clays. Note that very indurated lithologies were also recovered in the lacustrine facies of Imrali and are present at or immediately above the lacustrine–marine transition suggestive of exposure of the shelf. The calcium carbonate measured in the sediments ranges from 10 to 40% and it reached its greatest weight percent near or at the marine–lacustrine transition (Fig. 13).

3.8. Benthic and planktonic foraminifers

Following the submersion of the shelf edges at ~12 ka BP, *C. carinata* was the first abundant marine benthic foraminifer to appear in the sedimentary succession (Fig. 11). The occurrence of marsh and shallow water *A. tepida* and *Elphidium* spp. (*E. crispum*, *E. articulatum*, *E. macellum*) at 11.75 ka BP (10.6 ^{14}C ka BP) in Core 6, and 11.5 ka BP (10.5 ^{14}C ka BP) in Core 5, document the initial marine transgression. From 11.75 to 10.0 ka BP (10.6 to 9.3 ^{14}C ka BP) *C. carinata* is replaced first by *Brizalina* spp. (*B. catanensis*, *B. spathulata*) and then by *Bulimina* spp. dominated by *B. aculeata* (Fig. 11). After 10 kyr BP *A. tepida* and *Elphidium* spp. disappear as the shelf further submerges. Planktonic foraminifers appear in abundance. A very unusual 50 cm-thick deposit was found from 100 to 150 cm in Core 6 (Fig. 10). The sediments within this interval consist of homogeneous silty clays and contain fragments of marine mollusks and foraminifers. On the chirp records the deposit appears as a 2 m thick semi-transparent unit interpreted as a homogenite. Earthquakes have been linked to such deposits in the Marmara Sea. The strong shaking of slope sediments generated by an earthquake and seismically induced turbidity currents lead to the resuspension, dilution, and redeposition of fine-grained sediment the settles

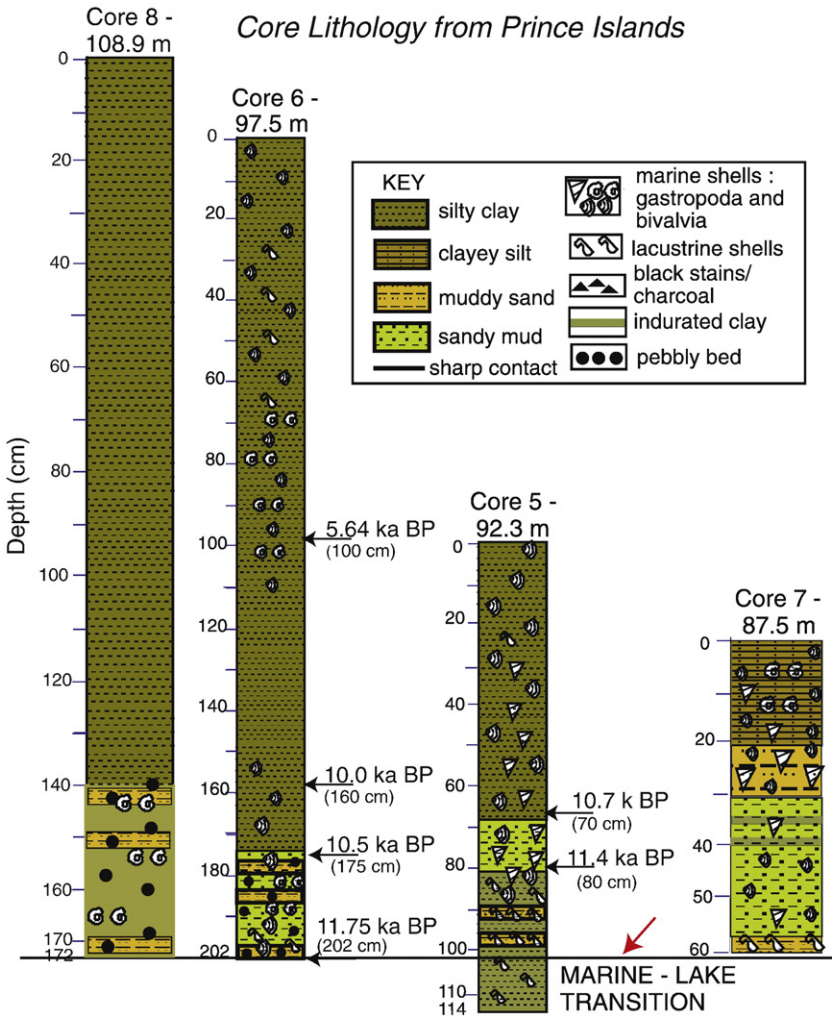

Fig. 10. Lithostratigraphic columns for Cores 8, 6, 5, and 7 recovered from the Prince Islands outer shelf. The sediments are generally sandy towards the base of the cores where they contain reworked lacustrine and marine shells indicating that the lacustrine–marine transition was very close but not penetrated by the cores possibly due to indurated or sandier strata. The sediments fine upwards to silty clays and contain marine faunas. Ages reported in calibrated years BP.

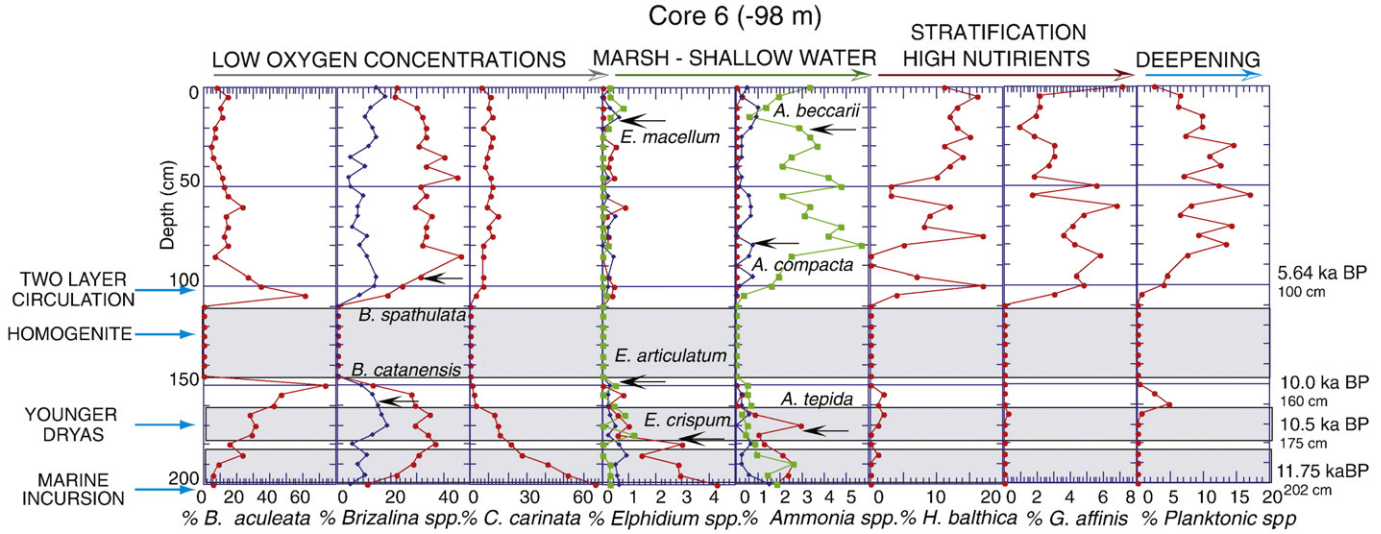

Fig. 11. Foraminiferal species in Core 6. The low oxygen concentration foraminifers are represented by *Bulimina* spp., *Brizalina* spp. and by *C. carinata*. *Bulimina aculeata* dominates *Bulimina* spp. and *Brizalina spathulata* and *Brizalina catanensis* dominate the *Brizalina* spp. As in Core IM05, *C. carinata* is the first colonizer after the marine incursion. The marsh shallow water foraminifers are represented by *Elphidium* spp. (*E. crispum*, *E. articulatum*, *E. macellum*) and *Ammonia* spp. (*A. tepida*, *A. compacta*, *A. beccarii*). After the initial marine incursion *A. tepida*, the marsh shallow water species, disappears and *Elphidium* spp. greatly diminishes in abundance. A homogenite deposit is present from 150 to 100 cm, Post 6 ka BP the environment becomes stable as shown by the lack of changes in foraminifers.

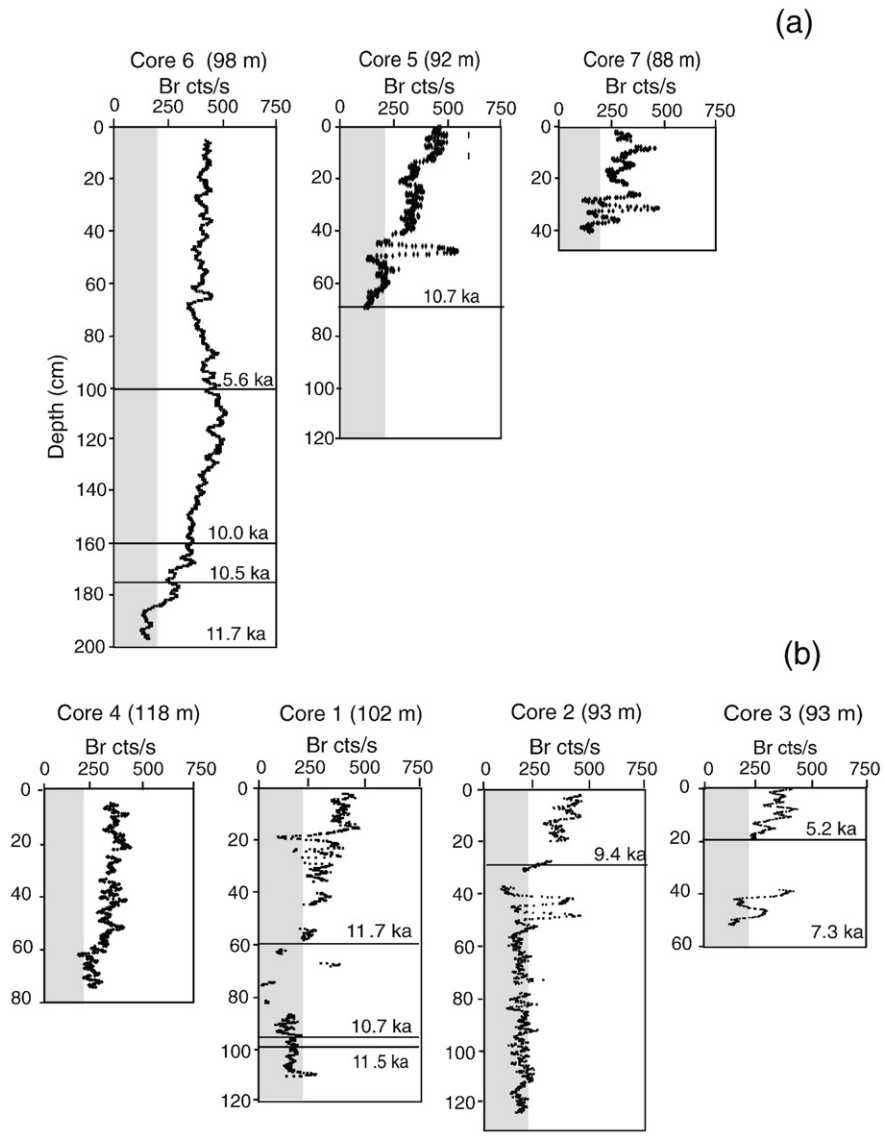

Fig. 12. Br content estimated from XRF scanning data (in counts/s). (a). Cores scanned from the Prince Islands shelf. (b). Cores scanned from the northern shelf (Çekmece). Values indicate freshwater-derived organic matter (less than 200 counts/s), whereas higher than that limit are indicative of marine organic matter. Calibrated dates at their corresponding levels in the cores are also shown.

to the sea-floor draping the basin and forming homogenous deposits (McHugh et al., 2006). A similar process where sediment was stirred and remained in suspension for several months and produced a homogeneous deposit was documented after the 1997 Cariaco Basin earthquake and the 1994 Sanriku-Oki earthquake (Thunell et al., 1999; Itou et al., 2000). After 6 ka BP the suboxic *C. carinata*, *Brizalina* spp. and *Bulimina* spp. remain stable in their relative abundances.

3.9. Northern shelf at Çekmece

The northern shelf of Marmara Sea at Çekmece was characterized by occurrences of three terraces located at −87 m, −93 m and −102 m of water depth (Fig. 14). Cores 4, 1, 2, and 3 were recovered from −118 m, −102 m, −93.3 m, and −93 m respectively. The limited penetration for Cores 3 and 4 suggests that they bottom a similar stiff, low-water content lacustrine facies as recovered in the IM05 core (Fig. 14). However, the mollusks *Dreissena* sp. and *Theodoxus* sp. reveal that lacustrine sediments were reached and recovered in limited thicknesses in Cores 1 and 2. The marine incursion was dated at 11.5 ka BP some 14 cm above the top of lacustrine sediments providing a minimum age for the event (Fig. 15). Lacustrine sediments were composed of clayey silts with abundant black stains and charcoal fragments. Low Br content (<200 counts/s) indicates that organic matter is not of marine origin in these sediments (Fig. 12). Unfossiliferous beds of indurated clays separated the lacustrine and marine sediments. The marine sediments in all cores are composed primarily of silty clays and sandy muds interrupted by occasional reworked intervals manifested by the mixed mollusk assemblages (marine, lacustrine) and by the ages that showed old above young (Cores 1 and 3; Fig. 14). The transition from lacustrine to marine sediments is characterized by a high variability in Br content that may be indicative of a variable marine–freshwater character of the basin, but more likely reflecting reworking and redeposition of sediments in the region (Fig. 12). Calcium carbonate weight percentage is greatest (up to 40 wt.%) within the lacustrine sediments and close to the lacustrine–marine transition but decreases up core (Fig. 13).

3.10. Benthic and planktonic foraminifers

Benthic foraminiferal assemblages showed very similar patterns as those from Imrali and Prince Islands (Fig. 16). *A. tepida* is present

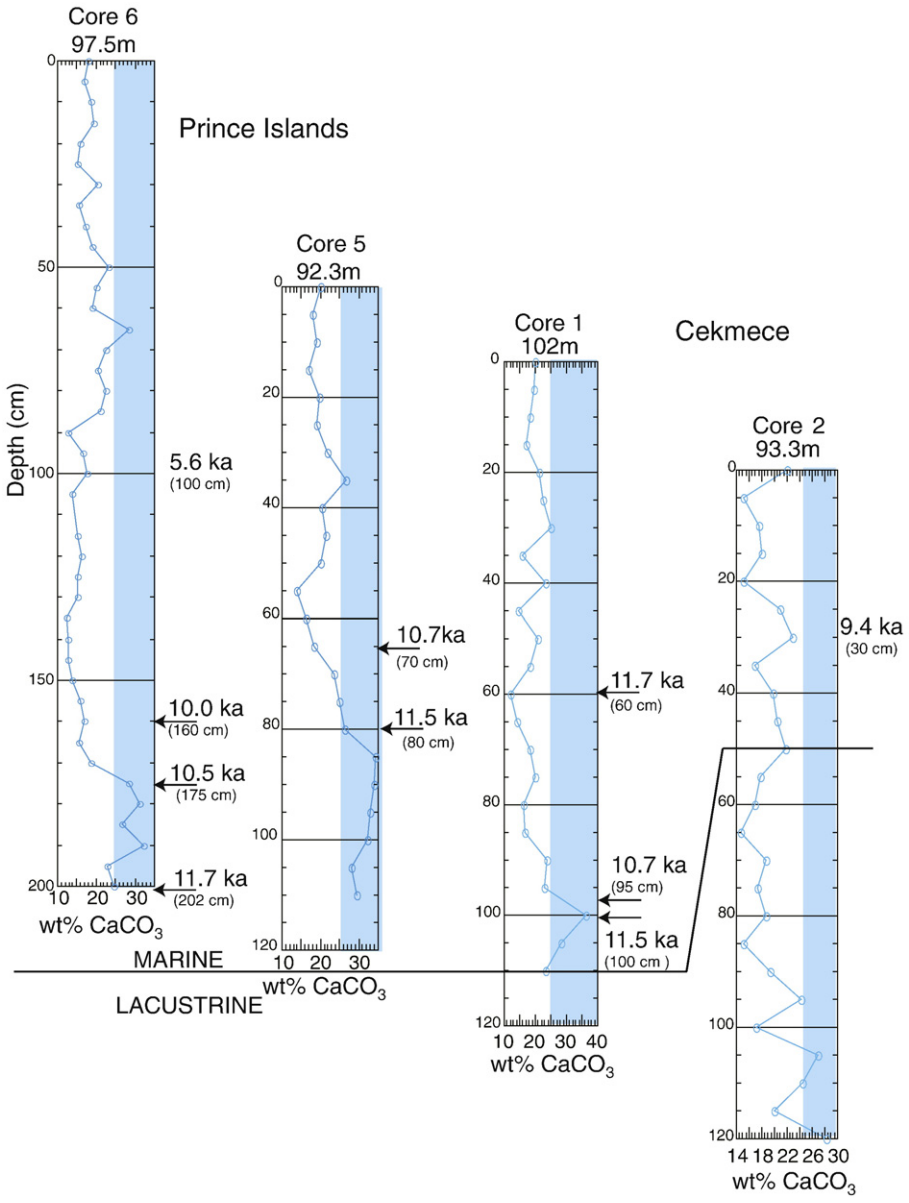

Fig. 13. Calcium carbonate wt.% for the Prince Islands and Çekmece cores. Values are greatest (25–40 wt.%) during the lacustrine stage and immediately above the marine incursion.

towards the base of the core with a prominent abundance peak at ~11.5 ka BP in Core 1 (−102 m). The abundance of *Elphidium* spp. decreases up core. *Bulimina* spp. and *Brizalina* spp. are dominated by *B. aculeata* and *B. spathulata*, respectively. From approximately 11.5 to 9.4 ka BP, *H. balthica* and *G. affinis* show peak abundances similar to those documented in the Imrali margin and interpreted as water stratification and nutrient influx possibly due to the Younger Dryas and Black Sea outflow. The part of the sedimentary record extending from 7.35 ka BP (6.9 ^{14}C ka BP) to the present showed a stable abundance of suboxic foraminifers with *Brizalina* spp. dominating the assemblages.

4. Discussion

The Marmara Sea has captured in its sediments, fauna and flora, paleoclimatic and paleoceanographic changes for approximately the past 15 ka BP (13.0 ^{14}C ka BP), at thousand-year scales, demonstrating how marginal basins are sensitive to changing paleoenvironmental conditions. The different proxies used (lithology, benthic and planktonic foraminifers, mollusk assemblages, diatoms, physical and geochemical properties and stable isotopes) permitted to track global sea-level as it breached the Dardanelles and Bosporus sills and reached its present position allowing for the Mediterranean, Marmara, and Black Sea waters to establish the present day circulation. The measured data allowed us to reconstruct a sequence of events described below (Fig. 17). The ages are listed as calibrated years for global comparison.

4.1. Marmara lacustrine stage (>15.5 ka BP to 12.0 ka BP)

The deglaciation of the Eurasia continental ice was initiated at 18.0 ka BP and extended until 15.8 ka BP (Bard et al., 1990; Grosswald 1980, 1998; Denton et al., 1999; Svitoch, 1999; Bahr et al., 2005). The effects of the Eurasia deglaciation can be expanded to the Black–Marmara Sea corridor until ~15.5 ka BP through a Caspian–Black Sea connection (Bahr et al., 2005). Once the initial disintegration of the Eurasian continental ice occurred, the retreating ice was not longer a source of meltwater to the Black Sea and consequently for the Marmara Lake (Bahr et al., 2005; Major et al., 2006). The oldest sediments recovered provide evidence of Marmara Lake isolated from the global ocean. The Lake sediments were laminated, indicative of

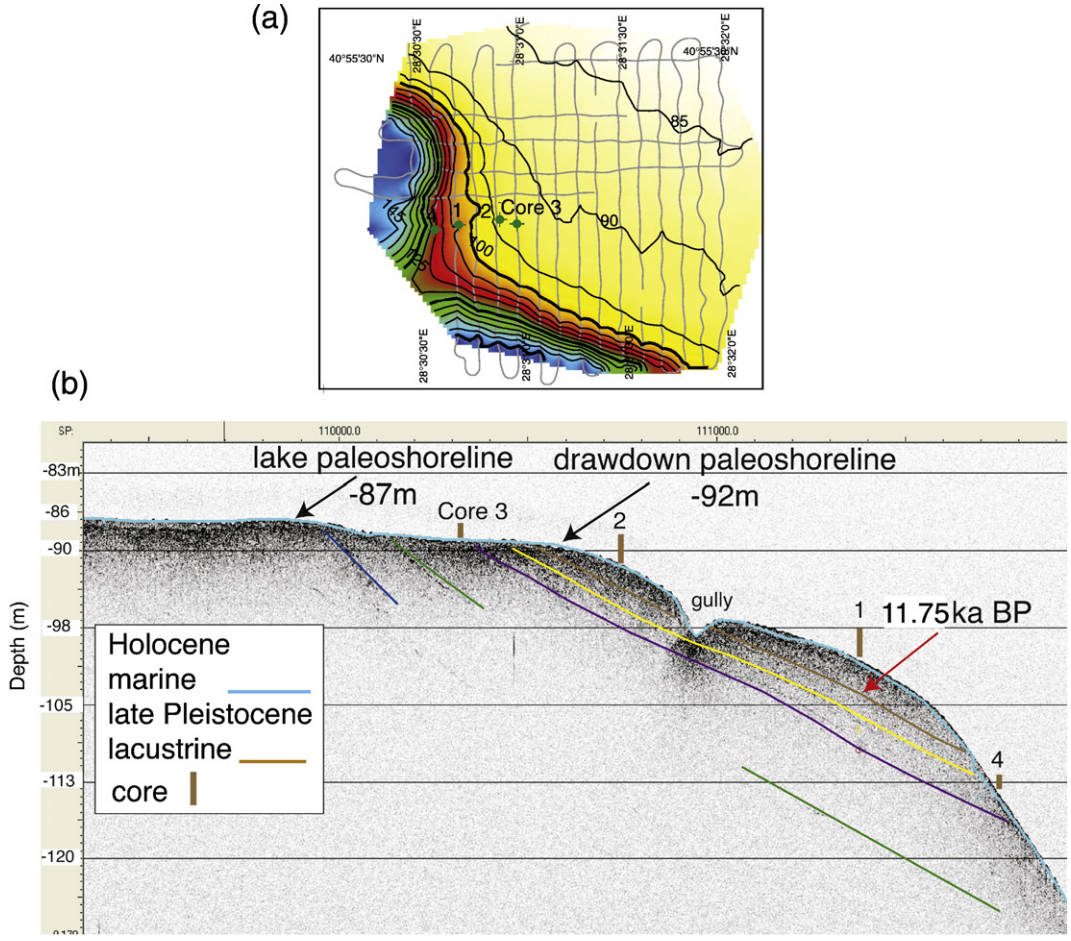

Fig. 14. (a). Water depth in meters and core location along the Çekmece outer shelf. (b). Subbottom profile (CHIRP) showing the −87 m high-stand lake paleoshoreline, a −92 m paleoshoreline, the late Pleistocene lacustrine surface (brown), and marine Holocene sediments above (turquoise surface).

cyclic sedimentation and oxic conditions (Fig. 4). Rivers were proximal bringing terrigenous sediment and the abundant charcoal suggested that the climate was dry with possible fires (Figs. 4, 15). The lake was nearly barren of fauna containing few *Dreissena* sp. and *Theodoxus* sp. of brackish and freshwater affinity, and rare brackish and fresh water diatom flora. The magnetic susceptibility data exhibits the greatest values during this barren lake stage. This signal is interpreted as derived from terrigenous sediments transported by rivers that drained into a proximal paleoshoreline (Fig. 6). Dry and cold climatic conditions and a sparsely vegetated landscape, which facilitated the erosion and transport of sediment by rivers, were documented for the Marmara and Black Sea regions at this time, except for the Black Sea southern coast, based on pollen stratigraphy (Caner and Algan, 2002; Filipova-Marinova et al., 2004; Mudie et al., 2001, 2007). From ~15.5 ka BP to 14.5 ka BP there is evidence for an abundant supply of fresh water from the Black Sea (a lake at this time) into Marmara Lake. The lake paleoshorelines lay at the level of its Dardanelles spillway to the Aegean Sea at −85 m, but isolated from the world's oceans (Lane-Serff et al., 1997; Çagatay et al., 2000; Algan et al., 2001; Aksu et al., 2002; Hiscott et al., 2002; Gökasan et al., 2008; Figs. 1, 17). Oligohaline conditions with salinities of 1–5‰ were present as documented by the Caspian-like mollusk assemblages (Fig. 4). *D. rostriformis* and *T. fluviatilis* were abundant. The $^{87}Sr/^{86}Sr$ compositions of these mollusks have a Black Sea signature (Major personal communication 2006; Major et al., 2006). The Bolling-Allerod interstadial brought warm conditions to Marmara Lake as manifested by the sediments, fauna, and flora of the lacustrine facies. Brackish and freshwater diatoms and woody material became less abundant just prior to the marine incursion when the magnetic susceptibility is high relative to marine values (Fig. 6).

4.2. Marine incursion—12 ka BP

The incursion of Mediterranean waters, at ~12.0 ka BP was accompanied by the replacement of the fauna and flora, the introduction of marine derived organic matter as manifested by Br counts/s, and a decrease in grain size and calcium carbonate abundance (Figs. 4–7, 12). All these changes were abrupt as measured by the thickness of the sediment over which the change occurred. This thickness is typically a few centimeters. It indicates that a transitional stage, if present was brief. The abruptness in the cores from both the northern and southern shelves contradicts the calculations of Myers et al. (2003) based on hydraulic theory which predicts a transition as long as 2.7 ka.

Paleoshorelines have been studied in Marmara Lake and used to reconstruct the geologic and climatic history of the region (Ergin et al., 1997; Çagatay et al., 1999, 2000, 2003). The −85 m terrace has been documented as the lake paleoshoreline at the level of its Dardanelles spillway with the Mediterranean Sea and the −65 m terrace as evidence for the Younger Dryas stillstand. The −95 m terrace documented in this study marks an erosional surface that can be traced nearly continuously throughout the Marmara Sea (Imrali, Prince Islands and Çekmece margins). The −95 m terrace, first documented by Aksu et al., 1999, lies almost 10 m below the Dardanelles bedrock sill. This raises the possibility that the levels of the lake dropped momentarily below the sill before the Mediterranean waters spilled into Marmara, or that

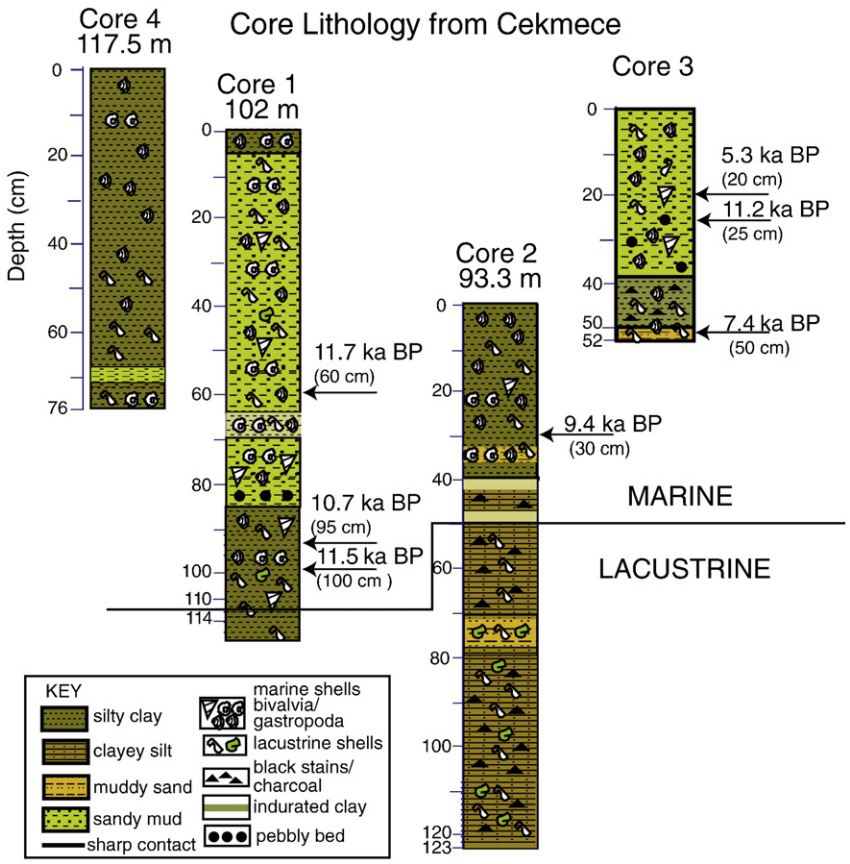

Fig. 15. Lithostratigraphic columns of cores taken in the northern Çekmece margin between −93 and −118 m of water depth. Mollusk assemblages (*Dreissena* sp., *Theodoxus* sp.) indicate lacustrine sediments in Core 2 from 50 to 123 cm and at the base of Core 1. Ages are reported in calibrated years BP. Lacustrine sediments are silt rich and contain charcoal fragments. Unfossiliferous layers of indurated clays, possibly diagenetically altered by carbonate cementation, separate the lacustrine and marine sediments. Marine sediments are primarily composed of silty clays with abundant marine mollusks and benthic and planktonic foraminifers. Cores 1 and 3 are sandier and contain reworked intervals manifested by the old over young ages and the mixing of marine and lacustrine shells.

wave action in the lake beveled the lake floor to form a terrace 10 m below the lake surface. The Bolling-Allerod, prior to 12 ka BP, was warm and hence evaporation rates were perhaps high enough to draw down the lake below its outlet. According to Major et al. (2006), the Black Sea responded similarly, expanding when cool and shrinking when warm.

Evaporative conditions of Marmara Lake and early Marmara Sea could explain salinity values of 4‰ greater than modern values calculated from alkenone measurements by Sperling et al. (2003). The earliest marine sediments have the heaviest oxygen isotope signal (2.3‰ $\delta^{18}O\delta^{18}O$; Fig. 8). An evaporative drawdown of the lake and

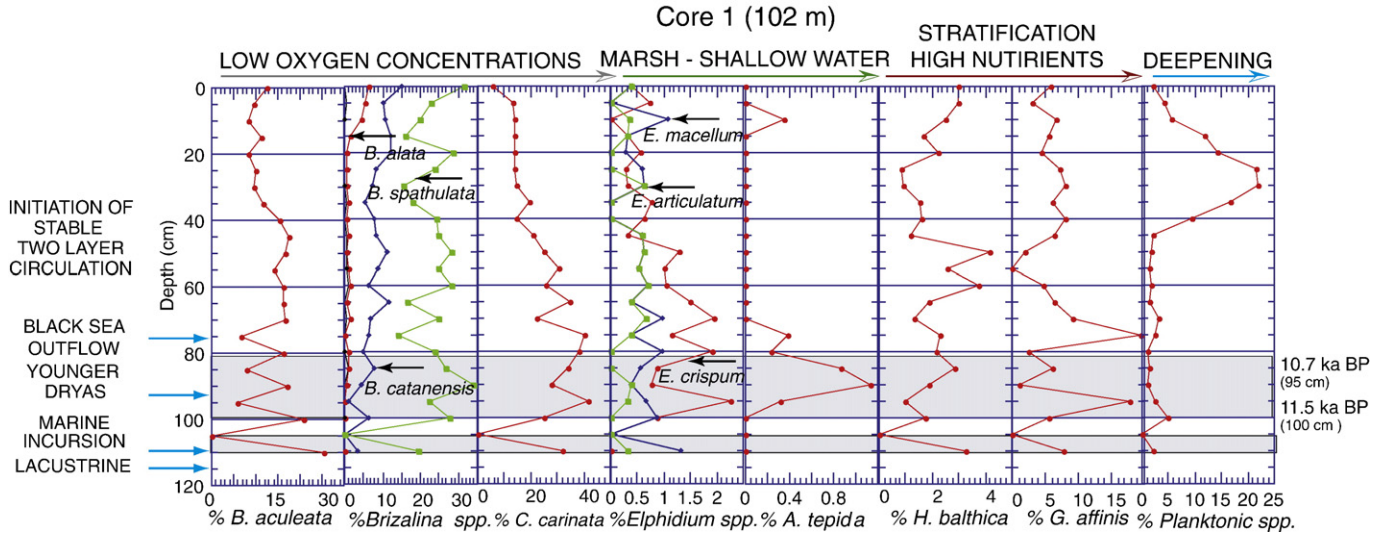

Fig. 16. Benthic and planktonic foraminiferal assemblages from the Çekmece outer shelf exhibit similar ecological shifts as those of Imrali and Prince Island shelves. Core 1 as in Core 6 shows the low oxygen concentration foraminifers dominated by *B. aculeata*, *B. spathulata*, *B. catanensis*, and *C. carinata*. A marsh shallow water environment is indicated by *A. tepida* and *E. crispum* that dominates the *Elphidium* spp. *Hyalinea balthica* and *Globobulimina affinis* show shifts in their abundance from approximately 11.5 to 8.2 ka BP possibly related to the Younger Dryas and Black Sea outflow.

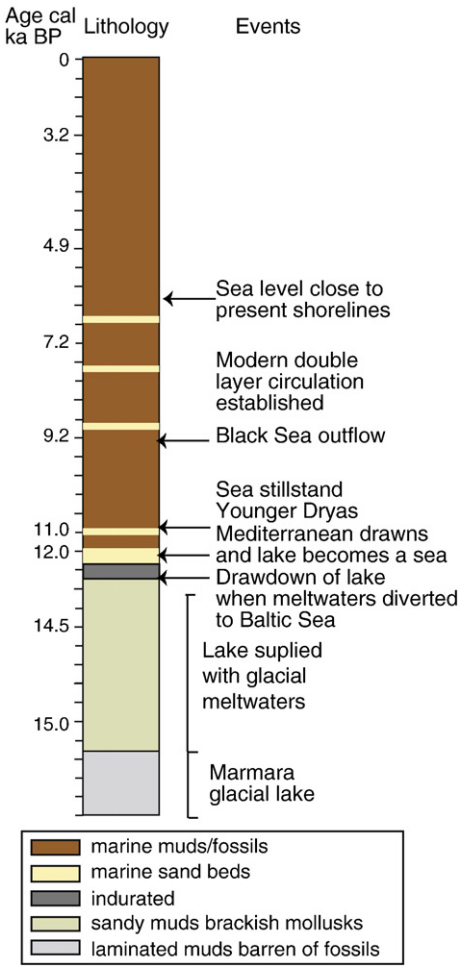

Fig. 17. Summary of the lithostratigraphy and biostratigraphy correlated to a calibrated radiocarbon chronology permits to reconstruct a sequence of events for the Black Sea–Marmara–Mediterranean corridor as documented by this study. The bases of the lithostratigraphic sequences provide evidence for Marmara Lake during glacial times. From ~15.5 ka BP to 14.5 ka BP the lake was supplied with glacial meltwaters from the Black Sea (a lake at this time) that spilled into the Marmara Lake and into the Aegean Sea. The Bolling-Allerod brought warm conditions to Marmara Lake from ~14.5 ka to 13.0 ka. Evaporative conditions prior to the marine incursion could have contributed to a lake drawdown with formation of the −95 m terrace, which could have also been formed by wave erosion. The incursion of marine waters into Marmara Sea occurred at 12 ka BP. At this time the Black Sea was either isolated or provided a very weak outflow to Marmara Sea. A standstill was documented from ~11.5 to 10.5 ka BP and interpreted as the Younger Dryas event. Sea-level continued to rise and there is evidence for strong outflow from the Black Sea at ~9.2 ka BP. The modern two-layer circulation was well established by 6 ka BP when sea-level reached close to the present shoreline.

sub-aerial exposure of the shelf edge would leave a stiff and low-water content substrate sampled at a depth below the Dardanelles spillway.

Authigenic carbonate precipitation is a common process in lakes experiencing evaporation. High autigenic carbonate is abundant in the Black Sea terminal lacustrine succession (Bahr et al., 2005; Major et al., 2006). In the deeper and permanently submerged regions of the Marmara Sea an authigenic carbonate layer was dated at ~12.5–14.5 ka BP (11.3–13.0 ^{14}C ka BP; Reichel and Halbach, 2007). Gypsum crystals were first reported by Stanley and Blanpied (1987) in the sediments of this age. The shelf muds we measured of the same age contain up to 40% carbonate (Fig. 13). Further work is needed to distinguish autigenic carbonate from the calcite of mollusk shells.

4.3. Younger Dryas 11.5–10.5 ka BP

The global transition from glacial to interglacial was interrupted by the Younger Dryas cold interstadial (Mangerud et al., 1974; Fairbanks 1989). Our data indicates that the Younger Dryas occurred in the Marmara Sea soon after the marine incursion. A fresh water outflow from the Black Sea into Marmara Sea could have been active during the Younger Dryas as proposed by Major et al. (2002) but there is uncertainty as to weather it was vigorous (Çagatay et al., 2000; Algan et al., 2001; Aksu et al., 2002; Hiscott et al., 2002; Major et al., 2002; Eris et al., 2007), or weak (Myers et al., 2003; Major et al., 2006). There is evidence of scour on the shelf at this time because we occasionally find older shells above younger shells, all in the age range of 11.5 to 10.5 ka BP. There is evidence that the −65 m terrace in the Izmit Gulf was formed during a Younger Dryas (Çagatay et al., 2003; Newman 2003). A still stand of sea-level was likely during the Younger Dryas, previously identified as the most arid period of the Last Glacial Age for the Eastern Mediterranean and the near East based on pollen data (Rossignol-Strick, 1995; Filipova-Marinova et al., 2004; Mudie et al., 2007).

4.4. Black Sea and Marmara Sea mixing of waters 9.4–9.2 ka BP

The timing and mode of reconnection between the Mediterranean, Marmara, and Black Sea have been heavily contested. Some studies proposed a non-catastrophic and gradual connection between the Mediterranean–Black Sea corridor (i.e., Aksu et al., 2002; Hiscott et al., 2002, 2006) while others proposed an abrupt and rapid process (i.e., Ryan et al., 1997, 2003; Major et al., 2002, 2006; Myers et al., 2003; Sidall et al., 2004; Giosan et al., 2005). The detailed analyses of benthic and planktonic foraminiferal assemblages from Marmara Sea shelves have provided additional insights into how the Black Sea connection occurred. It is well established that modern and ancient continental shelf waters undergo changes from oxic to anoxic conditions due to seasonal fluctuations in temperature and salinity, and as a result of longer-term climatic variability (Tyson and Pearson, 1991). Due to their rapid response, benthic foraminifers can document these ecological changes (Tyson and Pearson, 1991; Sen Gupta and Machain-Castillo, 1993; Sen Gupta et al., 1996; Kaiho, 1994; Kaminski et al., 2002). Global sea-level curves show that from 9.0 to 6.6 ka BP sea-level was −50 to −15 m below present (Fairbanks, 1989). This means that the shelf edges were sufficiently submerged to be able to experience variations in ventilation (Figs. 7, 11, 16). Increases in the occurrence of benthic foraminifers *H. balthica* and *G. affinis* were recorded as pulses in which their abundance increased from 0 to 30% (Figs. 7, 16). We interpret these pulses beginning at 9.2 ka BP as a manifestation of water stratification and high nutrients due to Black Sea outflow and the establishment of a two-layer circulation (Schonfeld, 1997, 2001; den Dulk et al., 2000; Evans et al., 2002; Fontanier et al., 2002, 2003; Murray 2006; Major et al., 2006). Later pulses in the abundance of *H. balthica* and *G. affinis* at ~7.6 and 6.6 ka BP can be explained as changes in organic matter flux that influenced biotic competition with resulting dominance of one fauna over another (Fig. 7).

4.5. Sea-level reaching the present shoreline—6 ka BP

The stable environmental conditions that developed as sea-level reached close to its present position at 6.0 ka BP were manifested by the lack of change in the abundance of both benthic and planktonic foraminiferal assemblages, the oxygen and carbon isotope records, and the physical properties of the sediments (Figs. 6–8, 11, 16). A two-layer circulation was well established by this time with *Brizalina* spp. dominating the low oxygen concentration forms. There were no major changes in water stratification and flux of organic mater as manifested by the lack of variability in *H. balthica* and *G. affinis*. Only the highly adaptable *A. beccarii* appears during this time. This species is known to be an opportunistic in other settings (Thomas et al., 2000). Sedimentation continued in the Marmara Sea at a steady rate of 0.02 cm/yr (Fig. 5). A slight decrease in the abundance of planktonic foraminiferal assemblages was observed at the Imrali,

Çekmece, and Prince Islands shelves (Figs. 7, 11, 16). The decrease can be linked to a slight increase in the magnetic susceptibility of the sediments in Imrali, which may represent an increase in magnetic minerals due to terrigenous transport (Fig. 6). Increased sediment supply due to deforestation in the Bronze Age is a possible explanation for the decrease in the biogenic proportion of the sediment (Eris et al., 2007).

5. Conclusions

The Marmara Sea is a small intracontinental basin that recorded in its sediments fluctuations in climate and water exchange between the Mediterranean and Black Seas demonstrating that such settings can serve as high-resolution repositories of environmental change. Our cores captured the pre-12 ka BP lacustrine low stand, the onset of the marine incursion and the subsequent Holocene transgression. The Younger Dryas cold interstadial left a faunal signal and evidence of scouring and sediment reworking. The sediments and fauna record the Black Sea outflow beginning at 9.2 ka BP and the subsequent water column stratification as Marmara Sea established its two-layer circulation.

Acknowledgements

We are grateful to Andreas Weill and Eco-Ocean Association of Herzlyia, Israel for making the *R/V Mediterranean Explorer* survey possible. We also thank the Captain and crew of the *R/V Mediterranean Explorer* and *R/V Urania* for their expertise in the collection of the data. We are grateful to the Scientific Party of the *R/V Urania* and to Drs. Vachtman, Eris, Ulug and Sarikavak for their help during the expeditions. We thank Corinne Hartin and Dr. Karen Kohfeld for their help with analyses at Queens College. We thank Dr. Mustapha Ergin and an anonymous reviewer for their comments that helped to improve the manuscript. Support for the analyses was from NSF-OCE-0222139; OCE-9807266 and PSC-CUNY 69138-00 38. This is a Lamont-Doherty Earth Observatory publication number 7183.

Appendix A

The key species are listed in alphabetical order. The identification of the benthic foraminifera are carried out on the studies by Murray (1971), Yanko and Troitskaja (1987), Alavi (1988), Loeblich and Tappan (1988), Cimmerman and Langer (1991), Sgarella and Moncharmont Zei (1993), Kaminski et al. (2002), Hayward et al. (2003), and Meric et al. (2004).

Adelosina cliarensis (Heron-Allen & Earland, 1930)

1930 *Quinueloculina cliarenesis* Heron-Allen & Earland (p. 58, pl. 3, figs. 26, 31)

1991 *Adelosina cliarensis* (Heron-Allen & Earland) Cimerman and Langer (p. 26, pl. 18, figs. 1–4)

Ammonia compacta (Hofker, 1969)

1969 *Streblus compactus* Hofker (p. 99, figs. 242–243)

1987 *Ammonia compacta* (Hofker), Yanko and Troitskaja (p. 44, pl. 11, figs. 1–10)

2002 *Ammonia compacta* (Hofker), Kaminski et al. (pl. 5, Fig. 8)

Ammonia beccarii (Linné, 1758)

1758 *Nautilus beccarii* Linné, (p. 710, pl. 1, fig. 1a–c)

1971 *Ammonia beccarii* (Linné) Murray (p. 151, pl. 62, figs. 1–7)

Ammonia tepida (Cushman, 1926)

1926 *Rotalia beccarii* (Linné) var. *tepida* Cushman (1926, p. 79, pl. 1)

1991 *Ammonia tepida* (Cushman) Cimerman and Langer (p. 76, pl. 87, figs. 10–12)

2003 *Ammonia tepida* (Cushman) Hayward et al. (pl. 1, figs. 1–3)

Asterigerinata mamilla (Williamson, 1858)

1858 *Rosalina mamilla* Williamson (p. 54, pl. 4, figs. 109–111)

1971 *Asterigerinata mamilla* (Williamson) Murray (1971, p. 141, pl. 59, figs. 1–9)

1991 *Asterigerinata mamilla* (Williamson) Cimerman and Langer (p. 73, pl. 82, figs. 1–4)

Bigenerina nodosaria d'Orbigny, 1826

1826 *Bigenerina nodosaria* d'Orbigny (p. 261, pl. 11, figs. 9–12)

1993 *Bigenerina nodosaria* d'Orbigny Sgarrella and Moncharmont Zei (p. 164, pl. 4, fig. 12)

Brizalina alata (Seguenza, 1862)

1862 *Vulvulina alata* Seguenza (p. 115, pl. 2, fig. 5).

1991 *Brizalina alata* (Seguenza), Cimerman and Langer (p. 59, pl. 61, figs. 12–14)

Brizalina catanensis (Segunenza, 1862)

1862 *Bolivina catanensis* Segunenza, (p.113, 125, pl.2, fig. 3)

1993 *Bolivina catanensis* Segunenza, Sgarrella and Moncharmont Zei (p. 208, pl. 14, figs. 4–5)

2002 *Brizalina catanensis* (Segunenza), Kaminski et al. (pl. 2, fig. 11)

Brizalina spathulata (Williamson, 1858)

1858 *Textularia variabilis* var. *spathulata* Williamson (p. 76, pl. 6, figs. 164–165).

1991 *Brizalina spathulata* (Williamson), Cimerman and Langer (p. 60, pl. 62, figs. 3–5)

Brizalina striatula (Cushman 1922)

1922 *Bolivina striatula* Cushman (p. 27, pl. 3, fig. 10)

1991 *Brizalina striatula* (Cushman) Cimerman and Langer (p. 60, pl. 62, figs. 6–9)

2002 *Brizalina striatula* (Cushman) Kaminski et al. (pl. 2, Fig. 10)

Bulimina aculeate d'Orbigny, 1826

1826 *Bulimina aculeata* d'Orbigny (p. 269)

1993 *Bulimina aculeata* d'Orbigny, Sgarrella & Moncharmont Zei (p. 211, pl. 15, fig. 1)

Bulimina costata d'Orbigny, 1852

1852 *Bulimina costata* d'Orbigny (p. 194)

1993 *Bulimina costata* d'Orbigny Sgarrella and Moncharmont Zei (p. 211, pl. 15, fig. 3)

Bulimina elongata d'Orbigny, 1846

1846 *Bulimina elongata* d'Orbigny (p. 187, pl. 11, figs. 19–20)

1993 *Bulimina elongata* d'Orbigny Sgarrella and Moncharmont Zei (p. 211, pl. 15, fig. 10–11)

2002 *Bulimina elongate* d'Orbigny, Kaminiski et al. (pl. 3, fig. 4)

Bulimina marginata d'Orbigny, 1826

1826 *Bulimina marginata*, d'Orbigny (p. 269, pl. 12, figs. 10–12).

1991 *Bulimina marginata* d'Orbigny, Cimerman and Langer (1991, p. 62, pl. 64, figs. 9–11)

1993 *Bulimina marginata* d'Orbigny, Sgarrella and Moncharmont Zei (p. 212, pl. 15, figs. 5–7)

Cassidulina carinata Silvestri, 1896

1896 *Cassidulina laevigata* d'Orbigny var. *carinata* Silvestri, (p. 104, pl. 2, figs. 10a–c)

1971 *Cassidulina carinata* Silvestri, Murray (p. 187, pl. 78, figs. 1–5)

1993 *Cassidulina carinata* Silvestri, Sgarrella and Moncharmont Zei (p. 236, pl. 23, figs. 8–9)

Chilostomella mediterranensis Cushman & Todd, 1949

1949 *Chilostomella mediterranensis* Cushman & Todd (p. 92, pl. 15, fig. 25–26).

1993 *Chilostomella mediterranensis* Cushman & Todd, Sgarrella and Moncharmont Zei (p. 238, pl. 24, fig. 11)

Discorbinella bertheloti (d'Orbigny, 1839)

1839 *Rosalina bertheloti* d'Orbigny (p. 135, pl. 1, figs. 28–30)

1993 *Discorbinella bertheloti* (d'Orbigny), Sgarrella and Moncharmont Zei (p. 216, pl. 16, figs. 11–12)

2002 *Discorbinella bertheloti* (d'Orbigny, 1839), Kaminiski et al. (pl. 5, figs. 1–2)

Elphidium aculeatum (d'Orbigny, 1846)

1846 *Polystomella aculeate* d'Orbigny (p. 131, pl. 6, figs. 27–28)

1991 Elphidium aculeatum (d'Orbigny) Cimerman and Langer (p. 77, pl. 89, figs. 1–4)

Elphidium complanatum (d'Orbigny, 1839)

1839 *Polystomella complanata* d'Orbigny (p. 129, pl. 2, figs. 35–36)
1993 *Elphidium complanatum* (d'Orbigny) Sgarrella and Moncharmont Zei (p. 228, pl. 20, figs .9–10)
Elphidium crispum (Linné, 1758)
1758 *Nautilus crispus*, Linné (p. 709, pl. 1, fig. 2d–f)
1971 *Elphidium crispum* (Linné), Murray (p. 155, pl. 64, figs. 1–6)
1991 *Elphidium crispum* (Linné), Cimerman and Langer (p. 77, pl. 90, figs. 1–6)
Elphidium macellum (Fichtel & Moll, 1798)
1798 *Nautilus macellus* var. *beta* Fichtel & Moll (p .66, pl. 10, figs. e–g, h–k)
1991 *Elphidium macellum* (Fichtel & Moll) Cimerman and Langer (p. 78, pl. 89, fig. 9)
2002 *Elphidium macellum* (Fichtel and Moll), Kaminski et al. (pl. 5, Fig. 11)
Favulina hexagona (Williamson, 1848)
1848 *Entosolenia squamosa* (Montagu) var. hexagona-Williamson (p. 20, pl. 2, fig. 23)
1991 *Favulina hexagona* (Montagu) Cimerman and Langer (p. 55, pl. 58, figs. 8–9)
Fursenkonia acuta (d'Orbigny, 1846)
1846 *Polymorphina acuta* d'Orbigny (p. 234, pl. 13, figs. 4–5; pl. 14, figs. 5–7)
1993 *Fursenkoina acuta* (d'Orbigny) Sgarrella and Moncharmont Zei (p. 235, pl. 23, fig. 7)
2002 *Fursenkonia acuta* (d'Orbigny), Kaminski et al. (pl. 3, figs. 11–12)
Globobulimina affinis (d'Orbigny, 1839)
1839 *Bulimina affinis* d'Orbigny (p. 105, pl. 2, figs. 25–26)
1993 *Globobulimina affinis* (d'Orbigny), Sgarrella and Moncharmont Zei (p. 212, pl.15, figs. 8–9)
2002 *Globobulimina affinis* (d'Orbigny), Kaminski et al. (pl. 3, Fig. 8)
Globocassidulina subglobosa (Brady, 1884)
1884 *Cassidulina subglobosa* Brady (p. 430, pl. 54, fig. 17a–c)
1971 *Globocassidulina subglobosa* (Brady), Murray (p. 191, pl. 80, figs. 1–4)
1991 *Globocassidulina subglobosa* (Brady), Cimerman and Langer (p. 61, pl. 63, figs. 4–6)
Haynesina depressula (Walker & Jacob, 1798)
1798 *Nautilus depressulus* Walker and Jacob (p. 641, figs. 33)
1971 *Nonion depressulum* (Walker and Jacob) Murray (p. 195, pl. 82, figs. 1–8)
2002 *Haynesina depressula* (Walker and Jacob) Kaminski et al. (pl. 4, figs. 4–5)
Hyalinea balthica (Schröter, 1783)
1783 *Nautilus balthicus* Schroter (p. 20, pl. 1, Fig. 2)
1993 *Hyalinea baltica* (Schroter) Sgarrella and Moncharmont Zei (p. 234, pl. 22, Fig. 12)
2002 *Hyalinea baltica* (Schroeter) Kaminski et al. (pl. 3, Fig. 13)
2004 *Hyalinea balthica* (Schroter) Meric et al. (pl. 27, Fig. 3)
Lagena striata (d'Orbigny, 1839)
1839 *Oolina striata* d'Orbigny (p. 21, pl. 5, fig. 12)
1991 *Lagena striata* (d'Orbigny) Cimerman & Langer (p. 53, pl. 55, figs. 6–7)
1993 *Lagena striata* (d'Orbigny) Sgarrella and Moncharmont Zei (p.198, pl.12, figs. 2–3)
Lobatula lobatula (Walker and Jacob, 1798)
1798 *Nautilus lobatulus*, Walker and Jacob (p. 642, pl. 14, fig. 36)
1988 *Lobatula lobatula* (Walker and Jacob), Loeblich and Tappan (p. 168, pl. 637, figs. 10–13)
1991 *Lobatula lobatula* (Walker and Jacob), Cimerman and Langer (p. 71, pl. 75, figs. 1–4)
Nonionella opima Cushman, 1947
1947 *Nonionella opima*, Cushman (p. 90, pl. 20, figs. 1–3)
1991 *Nonionella opima* Cushman, Cimerman and Langer (p. 74, pl. 84, figs. 1–3)
Nonionella turgida (Williamson, 1858)
1858 *Rotalina turgida*, Williamson (p. 50, pl. 4, figs. 95–97)
1971 *Nonionella turgida* (Williamson), Murray (p. 193, pl. 81, figs. 1–5)
1991 *Nonionella turgida* (Williamson), Cimerman and Langer (p. 74, pl. 84, figs. 6–8)
Planorbulina mediterranensis d'Orbigny 1826
1826 *Planorbulina mediterranensis* d'Orbigny (p. 280, no. 2)
1988 *Planorbulina mediterranensis* d'Orbigny, Loeblich and Tappan (p. 170, pl. 645, figs. 1–2)
1991 *Planorbulina mediterranensis* d'Orbigny, Cimerman and Langer (p. 71–72, pl. 78, figs. 1–8)
Quinqueloculina seminulum (Linné, 1758)
1758 *Serpula seminulum* Linné (p. 786, pl. 2, Fig. 1-a–c)
1971 *Quinqueloculina seminulum* (Linné) Murray (p. 64, pl. 24, figs. 1–6)
1991 *Quinqueloculina seminula* (Linné), Cimerman and Langer (p. 38, pl. 34, figs. 9–12)
Rectuvigerina phlegeri Le Calvez, 1959
1959 *Rectuvigerina phlegeri* Le Calvez (p. 363, pl. 1, fig. 11)
1988 *Rectuvigerina phlegeri* Le Calvez, Alavi (pl. 1, fig. 4)
1993 *Rectuvigerina phlegeri* Le Calvez, Sgarrella and Moncharmont Zei (p. 215, pl. 16, figs. 3–4)
Spiroloculina excavata d'Orbigny, 1846
1846 *Spiroloculina excavata* d'Orbigny, (p. 271, pl. 16, figs. 19–21)
1991 *Spiroloculina excavate* d'Orbigny, Cimerman and Langer (p. 30, pl. 23, figs. 1–3)
2002 *Spiroloculina excavata* d'Orbigny, Kaminski et al. (pl. 1, fig. 11)
Textularia bocki Höglund, 1947
1947 Höglund (p. 171, pl. 12, figs. 5–6)
1991 *Textularia bocki* Höglund, Cimerman and Langer (p. 21, pl. 10, figs. 3–6)
2002 *Textularia bocki* Höglund, Kaminski et al. (pl. 1, figs. 1–2)
Uvigerina mediterranea Hofker, 1932
1932 *Uvigerina mediterranea* Hofker (p. 118, p. 119, text figs. 32a–g)
1988 *Uvigerina mediterranea* Hofker Alavi (pl. 2, fig. 1)
1993 *Uvigerina mediterranea* Hofker, Sgarrella and Moncharmont Zei (p. 214, pl. 16, fig. 1–2)
Valvulineria bradyana (Fornasini, 1900)
1900 *Discorbina bradyana* Fornasini (p. 393, fig. 43)
1991 *Valvulineria bradyana* (Fornasini) Cimerman and Langer (p. 64, pl. 67, figs. 8–10)
1993 *Valvulineria bradyana* (Fornasini), Sgarrella and Moncharmont Zei (p. 220, pl. 18, figs. 1–2)

Appendix B. Supplementary data

Supplementary data associated with this article can be found, in the online version, at doi:10.1016/j.margeo.2008.07.005.

References

Abbott, R.T., Dance, S.P., 1990. Compendium of seashells: a color guide to more than 4,200 of the world's marine shells, 4th Edition. American Malacologists, Melbourne, Florida, USA. 411 pp.
Aksu, A.E., Hiscott, R.N., Yasar, D., 1999. Oscillating Quaternary water levels of the Marmara Sea and vigorous outflow into the Aegean Sea from the Marmara Sea–Black Sea drainage corridor. Mar. Geol. 153, 275–302.
Aksu, A.E., Hiscott, R.N., Kaminski, M.A., Mudie, P.J., Gillespie, H., Abrajano, T., Yasar, D., 2002. Last glacial–Holocene paleoceanography of the Black Sea and Marmara Sea: stable isotopic, foraminiferal and coccolith evidence. Mar. Geol. 3160, 1–31.
Alavi, S.N., 1988. Late Holocene deep-sea benthic foraminifera from the Sea of Marmara. Mar. Micropaleontol. 13, 213–237.
Algan, O., Çagatay, N., Tchepalyga, A., Ongan, D., Eastone, C., Gokasan, E., 2001. Stratigraphy of the sediment infill in Bosphorus Strait: water exchange between the Black and Mediterranean Seas during the last glacial Holocene. Geo Mar. Lett. 20, 209–218.
Armijo, R., Meyer, B., Hubert, A., Barka, A.A., 1999. Westward propagation of the north Anatolian fault into the northern Aegean: timing and kinematics. Geology 27, 267–270.
Armijo, R., Meyer, B., Navarro, S., King, G.C.P., Barka, A.A., 2002. Asymmetric slip partitioning in the Sea of Marmara pull-apart: a clue to propagation processes of the North Anatolian Fault? Terra Nova 14, 80–86.

Armijo, R., Pondard, N., Meyer, B., Uçarkus, G., Mercier de Lepinay, B., Malavieille, J., Dominguez, S., Gustcher, M.-A., Schmidt, S., Beck, C., Çagatay, M.N., Çakir, Z., Imren, C., Eris, K., Natalin, B., Özalaybey, S., Tolun, L.G., Lefèvre, I., Seeber, L., Gasperini, L., Rangin, C., Emre, Ö., Sarikavak, K., 2005. Submarine fault scarps in the Sea of Marmara pull-apart (North Anatolian Fault): implications for seismic hazard in Istanbul. Geochem. Geophys. Geosyst. 6, Q06009.

Bahr, A., Lamy, F., Arz, H., Kuhlmann, H., Wefer, G., 2005. Late glacial to Holocene climate and sedimentation history in the NW Black Sea. Mar. Geol. 214, 309–322.

Bard, E., Hamelin, B., Fairbanks, R.G., Zindler, A., 1990. Calibration of the 14C timescale over the past 30,000 years using mass spectrometric U–Th ages from Barbados corals. Nature 345, 405–410.

Behl, R.J., Kennett, J.P., 1996. Brief interstadial events in the Santa Barbara Basin, NE Pacific, during the past 60 kar. Nature 379, 243–246.

Besiktepe, S.T., Sur, H.I., Ozsoy, E., Latif, M.A., Orguz, T., Unluata, A., 1994. The circulation and hydrography of the Marmara Sea. Prog. Oceanogr. 34, 285–334.

Çagatay, M.N., Algan, O., Sakinç, M., Eastoe, C.J., Egesel, L., Balkis, N., Ongan, D., Caner, H., 1999. A mid–late Holocene sapropelic sediment unit from the southern Marmara sea shelf and its paleoceanographic significance. Quat. Sci. Rev. 18, 531–540.

Çagatay, M.N., Görür, N., Algan, A., Eastoe, C.J., Tchapalyga, A., Ongan, D., Kuhn, T., Kuscu, I., 2000. Late Glacial–Holocene palaeoceanography of the Sea of Marmara timing of connections with the Mediterranean and the black Sea. Mar. Geol. 167, 191–206.

Çagatay, M.N., Görür, N., Polonia, A., Demirbag, E., Sakinç, M., Cormier, M.-H., Capotondi, L., McHugh, C.M.G., Emre, Ö., Eris, K., 2003. Sea-level changes and depositional environments in the Izmit Gulf, eastern Marmara Sea, during the late glacial–Holocene period. Mar. Geol. 202, 159–173.

Caner, H., Algan, O., 2002. Palynology of sapropelic layers from the Marmara Sea. Mar. Geol. 190, 35–46.

Cannariato, K.G., Kennett, J.P., Behl, R.J., 1999. Biotic response to late Quaternary rapid climate switches in Santa Barbara Basin: ecological and evolutionary implications. Geology 27, 63–66.

Cimmerman, F., Langer, M.R., 1991. Mediterranean Foraminifera. Slovenska Akdemija Znanosti in Umetnosti. Classis IV: Historia Naturales dela Opera 30, Ljubljana. 119 pp., 93 pls.

Cormier, M.-H., Seeber, L., McHugh, C.M.G., Polonia, A., Çagatay, M.N., Emre, O., Gasperini, L., Görür, N., Bortoluzzi, G., Bonatti, E., Ryan, W.B.F., Newman, K., 2006. The North Anatolian fault in the Gulf of Izmit (Turkey): rapid vertical motion in response to minor bends of a non-vertical continental transform. J. Geophys. Res. 111. doi:10.1029/2005JB003633 B04102.

Demirbag, E., Rangin, C., LePichon, X., Sengör, A.M.C., 2003. Investigation of the tectonics of the Main Marmara Fault by means of deep-towed seismic data. Tectonophysics 361, 1–19.

Denton, G.H., Heusser, C.J., Lowell, T.V., Moreno, P.I., Anderson, B.G., Heusser, L.E., Schluchter, C., Marchant, D.R., 1999. Interhemispheric linkage of paleoclimate during the last glaciation. Geogr. Ann. 81, 107–153.

Debenay, J.-P., Benetau, E., Zhang, J., Stouff, V., Geslin, E., Redois, F., Fernandez-Gonzalez, M., 1998. Ammonia beccarii and Ammonia tepida (Foraminifera); morphofunctional arguments for their distinction. Mar. Micropaleontol. 34 (3), 235–244.

den Dulk, M., Reichart, G.J., van Heyst, S., van der Zwaan, G.J., 2000. Benthic foraminifera as proxies of organic matter flux and bottom water oxygenation? A case history from the northern Arabian Sea. Palaeogeogr. Palaeoclimatol. Palaeoecol. 161, 337–359.

Ergin, M., Bodur, M.N., Ediger, V., 1991. Distribution of surficial shelf sediments in the northeastern and southwestern parts of the Sea of Marmara: strait and canyon regimes of the Dardanelles and Bosporus. Mar. Geol. 96, 313–340.

Ergin, M., Nizamettin, K., Baki, V., Ozden, I., Levent, K., 1997. Sea-level changes and related depositional environments on the southern Marmara Shelf. Mar. Geol. 140, 391.403.

Eris, K.K., Ryan, W.B.F., Çagatay, M.N., Sancar, U., Lercolais, G., Menot, G., Bard, E., 2007. The timing and evolution of the post-glacial transgression across the Sea of Marmara shelf south of Istanbul. Mar. Geol. 243, 57–76.

Evans, J.R., Austin, W.E.N., Brew, D.S., Wilkinson, I.P., Kennedy, H.A., 2002. Holocene shelf sea evolution offshore northeast England. Mar. Geol., 191, 147–164.

Fairbanks, R.G., 1989. A 17,000-year glacio-eustatic sea level record: influence of glacial melting rates on the Younger Dryas event and deep-ocean circulation. Nature 342, 637–642.

Fedorov, P.V., 1971. Postglacial transgression of the Black Sea. Int. Geol. Rev. 14, 160–164.

Filipova-Marinova, M., Chirstova, R., Bozilova, E., 2004. Paleoecological conditions in the Bulgarian Black Sea area during the Quaternary. J. Environ. Micropaleontol. Microbiol. Meiobenthol. 1, 135–154.

Fontanier, C., Jorissen, F.J., Licari, L., et al., 2002. Live benthic foraminiferal faunas from the Bay of Biscay: faunal density, composition, and microhabitats. Deep-Sea Res. I 49, 751–785.

Fontanier, C., Jorissen, F.J., Chaillou, G., et al., 2003. Seasonal and interannual variability of benthic foraminiferal faunas at 550 m depth in the Bay of Biscay. Deep-Sea Res. I 50, 457–494.

Giosan, L., Mart, Y., McHugh, C.M., Vachtman, D., Çagatay, N.M., Kadir, E.K., Ryan, W.B., 2005. Megafloods in marginal basins: new data from the Black Sea. EOS Trans. AGU 86 (52), PP32A-03.

Gokasan, E., Demirbag, E., Oktay, F.Y., Ecevitoglu, B., Simsek, M., Yüce, H., 1997. On the origin of the Bosphorus. Mar. Geol. 140, 183–199.

Gökasan, E., Algan, O., Tur, H., Meriç, E., Türker, A., Simsek, M., 2005. Delta formation at the southern entrance of Istanbul Strait (Marmara sea, Turkey): a new interpretation based on high-resolution seismic stratigraphy. Geo Mar. Lett. 25, 370–377.

Gökasan, E., Ergin, M., Ozyalvac, M., Ibrahim Sur, H., Tur, H., Görum, T., Ustaömer, T., Gul Batuk, F., Alp, H., Birkan, H., Turker, A., Gezgin, E., Ozturan, M., 2008. Factors controlling the morphological evolution of the Canakkale Strait (Dardanelles, Turkey). Geo-Mar Letters 28, 107–129.

Görür, N., Çagatay, M.N., Sakinç, M., Sümengen, M., Sentürk, K., Yaltirak, C., Tchapalyga, A., 1997. Origin of the Sea of Marmara as deduced from Neogene to Quaternary Paleogeographic evolution of its frame. Int. Geol. Rev. 39, 342–352.

Grosswald, M.G., 1980. Late Weichselian ice sheet of Northern Europe. Quat. Res. 13, 1–32.

Grosswald, M.G., 1998. Late-Weichselian ice sheets in Arctic and Pacific Siberia. Quat. Int. 45–46, 3–18.

Gurung, D., McHugh, C.M., Ryan, W.B., Giosan, L., Mart, Y., Çagatai, N., 2006. Late Pleistocene–Holocene climate change inferred from fossil fauna in the Marmara Sea, Turkey. EOS Trans. AGU 87 (52), PP23B–1748.

Haynes, J.R., 1981. Foraminifera. John Wiley & Sons, New York. 433 pp.

Hayward, B., Buzas, M.A., Buzas-Stephens, P., Holzman, M., 2003. The lost types of *Rotalia Beccarii* var *tepida* Cushman 1926. J. Foraminiferal Res. 33, 352–354.

Hiscott, R.N., Aksu, A.E., Yasar, D., Kaminski, M.A., Mudie, P.J., Kostylev, V.E., MacDonald, J.C., Iser, F.I., Lord, A.R., 2002. Deltas south of the Bosphorus Strait record persistent Black Sea outflow to the Marmara Sea since ~10 ka. Mar. Geol. 190, 95–118.

Hiscott, R.N., Aksu, A.E., Mudie, P.J., Kaminski, M., Abrajano, T., Yasar, D., Rochon, A., 2006. The Marmara Sea Gateway since ~16 ka: non-catastrophic causes of paleoceanographic events in the Black Sea at 8.4 and 7.15 ka. In: Yanko-Hombach, V., Gilbert, A.S., Panin, N., Dolukhanov, P. (Eds.), The Black Sea Floor Question: Changes in Coastline, Climate and Human Settlement. Springer, Dordrecht, The Netherlands.

Hughen, K.A., Overpeck, L.C., Anderson, R.F., 1996. The nature of varved sedimentation in the Cariaco Basin, Venezuela, and its palaeoclimatic significance. In: Kemp, A.E.S. (Ed.), Palaeoclimatology and Palaeoceanography from Laminated Sediments. Geological Society, London, pp. 171–183.

Itou, M., Matsumura, I., Noriki, S., 2000. A large flux of particulate matter in the deep Japan Trench observed just after the 1994 Sanriku-Oki earthquake. Deep-Sea Res. I 4, 1987–1998.

Kaiho, K., 1994. Benthic foraminiferal dissolved-oxygen index and dissolved-oxygen levels in the modern ocean. Geology 22, 719–722.

Kaminski, M.A., Aksu, A., Box, M., Hiscott, R.N., Filipescu, S., Al-Salameen, M., 2002. Late Glacial to Holocene benthic foraminifer in the Marmara Sea: implications for Black Sea–Mediterranean Sea connections following the last deglaciation. Mar. Geol. 19, 165–202.

Lane-Serff, G.E., Rohling, E.J., Bryden, H., Charnock, H., 1997. Postglacial connection of the Black Sea to the Mediterranean and its relation to the timing of sapropel formation. Palaeoceanography 12, 169–174.

Lee, J.J., Pawlowski, J., Debenay, J.P., Whittaker, J.E., Banner, F.T., Gooday, A.J., Tendal, O., Haynes, J., Faber, W.W. 2000. Class Foraminifera In: J.J. Lee, G.F. Leedale, P. Bradbury (eds.). An Illustrated Guide to the Protozoa, 2nd Edition. Society of Protozoologists. Allen Press, Lawrence Kansas, 877–951.

Le Pichon, X., Sengör, A.M.C., Demirbag, E., Rangin, C., Imren, C., Armijo, R., Görür, N., Çagatay, M.N., Mercier de Lepinay, B., Meyer, B., Saatçilar, R., Tok, B., 2001. The active main Marmara fault. Earth Planet. Sci. Lett. 192, 595–616.

Leventer, A., Williams, D.F., Kennett, J.P., 1982. Dynamics of the Laurentide ice sheet during the last deglaciation: evidence from the Gulf of Mexico. Earth Planet. Sci. Lett. 59, 11–17.

Loeblich, A.R., Tappan, H., 1988. Foraminiferal genera and their classification, vol. 1–2. Van Nostrand Reinhold, New York. 970 pp., 847 pl.

Major, C.O., Ryan, W., Lercolais, G., Hajdas, I., 2002. Constraints on Black Sea outflow to the Sea of Marmara during the last glacial–interglacial transition. Mar. Geol. 190, 19–34.

Major, C.O., Goldstein, S.L., Ryan, W.B.F., Lercolais, G., Piotrowski, A.M., Hajdas, I., 2006. Quat. Sci. Rev. 25, 2031–2047.

Mangerud, J., Andersen, S.T., Berglund, B.E., Donner, J.J., 1974. Quaternary stratigraphy of Norden, a proposal for terminology and classification. Boreas 3, 109–127.

Malcolm, S.J., Price, N.B., 1984. The behaviour of iodine and bromine in estuarine surface sediments. Mar. Chem. 15, 263–271.

Mart, Y., Ryan, W., Çagatay, N., McHugh, C., Giosan, L., Vachtman, D., 2006. Evidence for intensive flow from the Bosporus northwards during the early Holocene. EGU Geophys. Res. Abstr. 8, 02572.

McHugh, C.M.G., Seeber, L., Cormier, M.-H., Dutton, J., Çagatay, M.N., Polonia, A., Ryan, W.B.F., Görür, N., 2006. Submarine earthquake geology along the North Anatolian Fault in the Marmara Sea, Turkey: a model for transform basin sedimentation. Earth Planet. Sci. Lett. 248, 661–684. doi:10.1016/j.epsl.2006.05.038.

Meric, E., Avsar, N., Bergin, F., 2004. Benthic foraminifera of Eastern Aegean Sea (Turkey) systematics and autoecology. Chamber of Geological Engineers of Turkey and Turkish Marine Research Foundation, 18. 306 pp.

Meric, E., Algan, O., 2007. Paleoenvironments of the Marmara Sea (Turkey) Coasts from paleontological and sedimentological data. Quat. Int. 167, 128–148.

Mudie, P.J., Aksu, A.E., Yasar, D., 2001. Late Quaternary dinoflagellate cysts from the Black, Marmara and Aegean seas: variations in assemblages, morphology and paleosalinity. Mar. Micropaleontol. 43, 155–178.

Mudie, P.J., Rochon, A., Aksu, A.E., 2002. Pollen stratigraphy of Late Quaternary cores from Marmara Sea: land–sea correlation and paleoclimatic history. Mar. Geol. 190, 233–260.

Mudie, P.J., Marret, F., Aksu, A.E., Hiscott, R.N., Gillespie, H., 2007. Palynological evidence for climatic change, anthropogenic activity and outflow of Black Sea water during the late Pleistocene and Holocene: centennial- to decadal-scale records from the Black and Marmara Seas. Quat. Int. 167, 73–90.

Murray, J.W., 1971. An Atlas of British Recent Foraminiferids. American Elsevier Publications, New York. 244 pp.

Murray, J.W., 1986. Living and dead Holocene foraminifera of Lyme Bay, Southern England. J. Foraminiferal Res. 16, 347–352.

Murray, J., 1991. Ecology and Palaeoecology of Benthic Foraminifer. Longman Scientific & Technical. 397 pp.

Murray, J., 2006. Ecology and Applications of Benthic Foraminifera. Cambridge University Press. 422 pp.

Myers, P.G., Wielki, C., Goldstein, S.B., Rohling, E.J., 2003. Hydraulic calculations of postglacial connections between the Mediterranean and the Black Sea. Mar. Geol. 201, 253–267.
Newman, K.R., 2003. Using Submerged Shorelines to Constrain Recent Tectonics in the Marmara Sea, Northwestern Turkey. Department of Geology, Senior Thesis, Smith College. 49 pp.
Okay, A.I., Demirbag, E., Kurt, H., Okay, N., Kusçu, I., 1999. An active, deep marine strike-slip basin along the North Anatolian fault in Turkey. Tectonics 18, 129–147.
Okay, N., Ergun, B., 2005. Source of basinal sediments in the Marmara Sea investigated using heavy minerals in the modern beach sands. Mar. Geol. 216, 1–15.
Ortiz, J.D., O'Connell, S.B., DelViscio, J., Dean, W., Carriquiry, J.D., Marchitto, T., Zheng, Y., vanGeen, A., 2004. Enhanced marine productivity off western North America during warm climate intervals of the past 52 k.y. Geology 32, 521–524.
Peterson, L.C., Overpeck, J.R., Kipp, N.G., Imbrie, J., 1991. A high-resolution late Quaternary upwelling record from the anoxic Cariaco Basin, Venezuela. Paleoceanography 6, 99–119.
Phleger, F., 1960. Ecology and Distribution of Recent Foraminifera. John Hopkins Press, Baltimore, MD. 297 pp.
Polonia, A., Cormier, M.H., Çagatay, M.N., Bortoluzzi, G., Bonatti, E., Gasperini, L., Seeber, L., Görür, N., Capotondi, L., McHugh, C.M.G., Ryan, W.B.F., Emre, O., Okay, N., Ligi, M., Tok, B., Blasi, A., Busetti, M., Eris, K., Fabretti, P., Fielding, E.J., Imren, C., Kurt, H., Magagnoli, A., Marozzi, G., Ozer, N., Penitenti, D., Serpi, G., Sarikavak, K., 2002. Exploring submarine earthquake geology in the Marmara Sea. EOS Transactions AGU 83 229, 235–236.
Polonia, A., Gasperini, L., Amorosi, A., Bonatti, E., Bortoluzzi, G., Çagatay, M.N., Capotondi, L., Cormier, M.-H., Görür, N., McHugh, C.M.G., Seeber, L., 2004. Holocene slip rate of the North Anatolian Fault beneath the Sea of Marmara. Earth Planet. Sci. Lett. 227, 411–426.
Rangin, C., Demirbag, E., Imren, C., Crusson, A., Normand, A., Le Drezen, E., Le Bot, A., 2001. Marine Atlas of the Sea of Marmara. Ifremer.
Reichel, T., Halbach, P., 2007. An authigenic calcite layer in the sediments of the Sea of Marmara—a geochemical marker horizon with paleoceanographic significance. Deep Sea Res. II 54, 1201–1215.
Renberg, I., 1990. A procedure for preparing large sets of diatom slides form sediment cores. J. Paleolimnol. 4, 87–90.
Ross, D.A., Degens, E.T., 1974. Recent sediments of the Black Sea. In: Degens, E.T., Ross, D.A. (Eds.), The Black Sea Geology. Chemistry and Biology, vol. 20. Am. Assoc. Petrol. Geol. Mem., Tulsa, pp. 183–199.
Rossignol-Strick, M., 1995. Sea–land correlation of pollen records in the eastern Mediterranean for the glacial–interglacial transition: Biostratigraphy versus radiometric time-scale. Quat. Sci. Rev. 14, 893–915.
Round, F.E.E., Crawford, R.M., Mann, D.G., 1990. Diatoms: Biology and Morphology of the Genera. Cambridge University Press. 560 pp.
Ryan, W.B.F., Pitman, W.C., Major, C.O., Shimkus, K., Moskalenko, V., Jones, G.A., Dimitrov, P., Görür, N., Sakinç, M., Yüce, H., 1997. An abrupt drowning of the Black Sea shelf. Mar. Geol. 138, 119–126.
Ryan, W.B.F., Major, C.O., Lericolais, G., Goldstein, S.L., 2003. Catastrophic flooding of the Black Sea. Annu. Rev. Earth Planet. Sci. 31, 525–554.
Schonfeld, J., 1997. The impact of the Mediterranean Outflow Water (MOW) on benthic foraminiferal assemblages and surface sediments at the southern Portuguese continental margin. Mar. Micropaleontol. 29, 211–236.
Schonfeld, J., 2001. Benthic foraminifera and pore-water oxygen profiles: a re-assessment of species boundary conditions at the western Iberian margin. J. Foraminiferal Res. 31, 86–107.
Sengör, A.M.C., Görür, N., Saroglu, F., 1985. Strike-slip faulting and related basin formation in zones of tectonic escape: Turkey as a case study, in Strike-Slip Deformation, Basin Formation, and Sedimentation. In: Biddle, K.T., Christie-Blick, N. (Eds.), Soc. Econ. Paleont. Min. , pp. 227–264.
Sen Gupta, B.K., Machain-Castillo, M.L., 1993. Benthic foraminifera in oxygen-poor habitats. Mar. Micropaleontol. 20, 183–201.
Sen Gupta, B.K., Turner, R.E., Rabalis, N.N., 1996. Seasonal oxygen depletion in continental-shelf waters of Louisiana—historical record of benthic foraminifers. Geology 24, 227–230.
Sgarella, F., Moncharmont Zei, M., 1993. Benthic foraminifera of the Gulf of Naples (Italy): Systematics and autoecology. Boll. Soc. Paleontol. Ital. 32, 145–264.
Sidall, M., Rohling, E.J., Almogi-Labin, A., Hemleben, Ch., Meischner, D., Schmelzer, I., Smeed, D.A., 2003. Sea-level fluctuations during the last glacial cycle. Nature 423, 853–858.
Sidall, M., Lawrence, J.P., Helfrich, K.R., Giosan, L., 2004. Testing the physical oceanographic implications of the suggested sudden Black Sea infill 8400 years ago. Paleoceanography 19, PA1024. doi:10.1029/2003PA000903.
Siani, G., Paterne, M., Arnold, M., Bard, E., Metivier, B., Tisnerat, N., Bassinot, F., 2000. Radiocarbon reservoir ages in the Mediterranean Sea and Black Sea. Radiocarbon 42, 271–280.
Sperling, M., Schmiedl, G., Hembleben, Ch., Emeis, K.C., Erlenkeuser, H., Grootes, P.M., 2003. Black Sea impact on the formation of eastern Mediterranean sapropel S1? Evidence from the Marmara Sea. Palaeogeogr. Palaeoclimatol. Palaeoecol. 190, 9–21.
Stanley, D.J., Blanpied, C., 1980. Late Quaternary water exchange between the eastern Mediterranean and the Black Sea. Nature 266, 537–541.
Stuvier, M., Reimer, P.J., 1993. Extended 14C database and revised CALIB radiocarbon calibration program. Radiocarbon 35, 215–230.
Svitoch, A.A., 1999. Caspian Sea level in the Pleistocene: hierarchy and position in the paleogeographic and chronological records. Oceanology 39, 94–101.
Thomas, E., Gapotchenko, T., Varekamp, J., Mecray, E.L., Buchholtz ten Brink, M.R., 2000. Benthic foraminifera and environmental changes in Long Island Sound. J. Coast. Res. 16, 641–655.
Thunell, R.C., Williams, D.F., 1989. Glacial–Holocene salinity changes in the Mediterranean Sea: hydrographic and depositional effects. Nature 338, 493–496.
Thunell, R., Tappa, E., Varela, R., Llano, M., Astor, Y., Muller-Karger, F., Bohrer, R., 1999. Increased marine sediment suspension and fluxes following an earthquake. Nature 398, 233–236.
Tyson, R.V., Pearson, T.H., 1991. Modern and ancient continental shelf anoxia: an overview. Geological Society Special Publication 58, 1–24.
Vaught, K.C., Abbott, R.T., Boss, K.J., 1989. Classification of the Living Mollusca. American Malacologist, Melbourne, Fla. U.S.A. 204 pp.
Yanko, V.V., Troitskaja, T.S., 1987. Pozdne-chetvertichnye foraminifery Chernogo morya. Late Quaternary Foraminifera of the Black Sea. Akademiya Nauk SSSR, 694. Institut Geologii I Geofiziki Trudy. 111 pp.